AN ABSTRACT OF THE THESIS OF

Richard Shih-Ming Lu (Name) for the Doctor of Philosophy (Degree)

in Geophysics (Major) presented on August 16, 1973 (Date)

Title: PERTURBATION METHODS IN GEOPHYSICS AND OCEANOGRAPHY

Abstract approved: Redacted for Privacy

Quinn Bouvarsson

The perturbation method is applied to solve two numerical problems in the earth sciences, viz., (1) the computation of deep sea currents in the coastal region of the northeast Pacific and (2) the interpretation of D.C. conduction data in exploration geophysics. The perturbation method is largely equivalent to the method of successive approximation. The variational method is also used in the study of the dynamics of the deep sea currents.

The deep sea currents in the coastal region of the northeast Pacific can be calculated approximately by solving the linearized equations for long waves in shallow basins. Both the perturbation and the variational methods are employed to solve these equations in the case of step shelf models approximating the shelf contours in the region. It is concluded that the perturbation method using the Fourier transform technique is to be preferred for the problem at

hand. The results show that the topography of the continental shelf and the continental slope has only a minor effect on the deep sea currents in the abyssal plain region.

In the case of the D.C. conduction exploration method, the perturbation method is applied both to the problem of computing the surface potential due to a given conductivity distribution and also to the inverse problem of interpreting given field data. The first case involves the solving of an ordinary second order differential equation by numerical methods followed by a numerical Hankel transformation. The inversion procedure involves, in particular, the numerical inversion of a Laplace transformation. The application of these methods to two- and three-layer cases is demonstrated by working out some examples. It is shown that the perturbation method can be applied with good results provided certain conditions are satisfied. The main practical difficulty is encountered in the numerical Laplace inversion which is an improperly posed problem.

Perturbation Methods in Geophysics and Oceanography

by

Richard Shih-Ming Lu

A THESIS

submitted to

Oregon State University

in partial fulfillment of
the requirements for the
degree of

Doctor of Philosophy

June 1974

APPROVED:

Redacted for Privacy

Professor of Geophysics and Mathematics

in charge of major

Redacted for Privacy

Dean of School of Oceanography

Redacted for Privacy

Dean of Graduate School

Date thesis is presented Aug 16 1973

Typed by Suelynn Williams for Richard Shih-Ming Lu

To

G. M. B.

ACKNOWLEDGMENTS

I thank Dr. Bodvarsson, my major professor for his guidance in the whole work of this thesis. His help and patience are deeply appreciated.

I wish to thank also Mr. D. Eggers for his help in the calculations of deep sea currents, Mr. K. Keeling for his help as a consultant of computer programming, and Ms. J. Gemperle for her help of drafting some of the figures.

Dr. R. Blakely, Dr. W. Fredericks, Dr. H. Goheen, Dr. D. Heinrichs, Dr. F. Oberhettinger and Dr. A. Wasserman serve on my committee, review my thesis and give valuable comments. For their assistance I am grateful.

The occasional talking and discussion with Dr. S. Newberger were rewarding and valuable.

I thank Mr. W. MacFarlane and Ms. G. Bodvarsson who proofread my thesis. The friendship and helpful discussion of the faculties and fellow students in the school of oceanography were also gratefully acknowledged.

Thanks are extended to my lovely parents, their prayers, support, and encouragement are essential to the completion of this thesis.

This work was supported by the National Science Foundation. During the period of this work I was a recipient of assistantships

from both the National Science Foundation and the Office of Naval Research. I am thankful for this assistance.

TABLE OF CONTENTS

LIST OF FIGURES

LIST OF FIGURES CONTINUED

LIST OF TABLES

PERTURBATION METHODS IN GEOPHYSICS AND OCEANOGRAPHY

INTRODUCTION

A General Description of the Perturbation and Variational Methods in Mathematics

Exact solutions of the differential or integral equation of applied mathematics can be obtained in only a relatively limited number of cases. For example, as mentioned by Morse and Feshbach (1953), the method of separation of variables to solve the scalar Helmholtz equation can be used only in 11 coordinate systems (see 5.1 of Morse and Feshbach, 1953). If the boundary surfaces do not coincide with these coordinate surfaces, or if the boundary conditions are not the simple Dirichlet or Neumann types, exact solutions cannot be derived. The same applies to integral equations. The kernel of the integral equation has to be of a certain specific form for exact solutions to be obtainable. Hence we are very frequently faced with the task of developing approximate methods to attack a given problem. Moreover, sometimes the derivation of the exact solution of an equation can be a very complicated operation; whereas the approximate technique is more convenient and therefore to be preferred.

In this thesis we demonstrate the application of two approximation methods, viz., the perturbation and the variational methods, to

the solution of problems in the earth sciences. The main emphasis is on the perturbation method which is applied (1) in the computation of deep sea currents in coastal areas of the northeast Pacific and (2) in the interpretation of D.C. conduction field data. A brief review of the perturbation and variational methods follows.

Perturbation Method. (Kato, 1966)

The perturbation method is based on the idea of approximating a given system by a simpler, ideal system which deviates only slightly from the system under consideration. The perturbation theory (from now on means the perturbation theory for linear operators) was originated by Rayleigh and Schrödinger (Rayleigh, 1926; Schrödinger, 1928). These early works were of an applied character and mathematically incomplete. It was not until Rellich (1937^1, 1937^2, 1939, 1940, 1942) published a series of papers that the questions of the existence and convergence of the perturbation method were settled satisfactorily. Theorems and criteria were provided for the applicability of the perturbation method to the problem with discrete spectra. The basic results of Rellich may be stated as follows: (Kato, 1966) Let $T(\varepsilon)$ be a bounded self-adjoint operator in a Hilbert space, depending on a real parameter ε and which can be expanded into a convergent power series

$$T(\varepsilon) = T + \varepsilon T^{(1)} + \varepsilon^2 T^{(2)} + \cdots . \qquad (1)$$

Suppose that the unperturbed operator $T = T(0)$ has an isolated eigenvalue λ (isolated from the rest of the spectrum) with a finite multiplicity m. Then $T(\varepsilon)$ has for sufficiently small $|\varepsilon|$ exactly m eigenvalues $\mu_j(\varepsilon)$, $j = 1, 2, \ldots, m$ (multiple eigenvalues counted repeatedly) in the neighborhood of λ. The eigenvalues can be expanded into convergent series

$$\mu_j(\varepsilon) = \lambda + \varepsilon \mu_j^{(1)} + \varepsilon^2 \mu_j^{(2)} + \cdots, \quad j = 1, 2, \ldots, m. \quad (2)$$

The associated eigenvectors $\varphi_j(\varepsilon)$ of $T(\varepsilon)$ can also be expanded into convergent series

$$\varphi_j(\varepsilon) = \varphi_j + \varepsilon \varphi_j^{(1)} + \varepsilon^2 \varphi_j^{(2)} + \cdots, \quad j = 1, 2, \ldots, m, \quad (3)$$

satisfying the orthogonality conditions

$$(\varphi_j(\varepsilon), \varphi_k(\varepsilon)) = \delta_{ik},$$

where the φ_j form an orthonormal family of eigenvectors of T for the eigenvalue λ. The existence and analyticity of $\mu_j(\varepsilon)$ and $\varphi_j(\varepsilon)$ are ensured by appropriate assumptions on T and ε.

Friedrichs (1938, 1948, 1965) developed the perturbation theory of continuous spectra which is very important in scattering theory, quantum field theory, and other applications. Titchmarsh (1949, 1950) and Kato (1951, 1966) have shown that the series (2) or (3) approximate the $\mu_j(\varepsilon)$ and $\varphi_j(\varepsilon)$ in the sense of asymptotic expansion even if the series are divergent. Thus the applicability of the

perturbation method is extended. Criteria have been given for the validity of the perturbation method in the sense of asymptotic expansion. (Titchmarsh, 1949, 1950; Kato, 1951, 1966)

These theorems have been proven in a very general sense. Their applications to the problems in quantum theory have been studied very carefully. Rigorous proofs for special cases are very difficult and beyond the scope of this presentation.

Variational Method. (Mikhlin, 1964)

In many cases the problems of integrating a differential equation can be replaced by an equivalent variational problem. For example, under general boundary conditions it is possible to reduce the integration of the equations of static elasticity theory to the deriving of a minimum of the potential energy of the elastic body (Mikhlin, 1964). The methods which allow us to reduce the problem of integrating a differential equation to some kind of a variational problem are usually called variational or energy methods.

One of the first variational methods in history was formulated in the form of the so called "Dirichlet principle". Based on this principle (if only the two-dimensional problem is considered) of all the functions with prescribed values on the boundary of some domain D, the function which gives the least value of the Dirichlet integral

$$\iint_D \left[\left(\frac{\partial u}{\partial x}\right)^2 + \left(\frac{\partial u}{\partial y}\right)^2 \right] \, dx \, dy$$

is harmonic in D. Weierstrass (1895) and Hadamard later gave examples which showed that the Dirichlet principle may not be strictly valid under certain very special circumstances. Thus the principle was in some doubt and was neglected for a long time. Interest in the Dirichlet principle and the variational method in general was aroused again through the work of Hilbert and of Ritz (1908, 1911). The later so called "Ritz method" which proved to be very useful is outlined below. The reader is referred to Courant and Hilbert (1953, 1962) and Mikhlin (1952, 1964) for a detailed treatment of the Ritz method which is a generalization of the Rayleigh method (Rayleigh, 1926).

When the operator A is positive definite, i.e., $(Au, u) > 0$ for every $u \neq 0$, and is symmetric, solving the equation

$$Au = f(P) \tag{4}$$

can be reduced to finding the minimum of the functional (Mikhlin, 1964):

$$F(u) = (Au, u) - 2(u, f) \, . \tag{5}$$

The approximate solution u_n is formulated as:

Let $\{\varphi_i(P)\} = \{\varphi_i(P),\ i = 1,\ 2,\ \ldots\ n \mid$ ① $\varphi_i(P) \in D_A$ (domain of A); ② sequence φ_i is complete in energy; ③ for any n, $\varphi_i(P)$, $\varphi_2(P)$, $\ldots$ $\varphi_n(P)$ are linearly independent$\}$ and

$$u_n = \sum_{j=1}^{n} a_j \varphi_j(P) \tag{6}$$

where a_j are numerical coefficients. Substituting (6) into (5) and requiring that

$$\frac{\partial F(u_n)}{\partial a_i} = 0 , \qquad i = 1, 2, \ldots, n$$

the equation

$$\sum_{k=1}^{n} (A\varphi_i, \varphi_k) a_k = (f, \varphi_i), \qquad i = 1, 2, \ldots, n$$

is obtained, from which the a_i's, $i = 1, 2, \ldots, n$ and consequently u_n are obtained.

The Bubnov-Galerkin method (Galerkin, 1919), which is a special case of the more general so called projection method is formulated as follows. Let the linear operator A in (4) above be defined for a set of functions which is dense in a separable Hilbert space. We select $\{\varphi_n\}$, $\varphi_n \in D_A$ and construct an approximate solution

$$u_n(P) = \sum_{k=1}^{n} a_k \varphi_k(P) \quad .$$

The constants a_k are then determined by the orthogonality conditions:

$$\sum_{k=1}^{n} (A\varphi_k, \varphi_j) a_k = (f, \varphi_j), \qquad j = 1, 2, \ldots, n \quad .$$

This method is more general than the Ritz method (Bubnov, 1913). The Bubnov-Galerkin method can be applied to both differential and integral equations. For the extent of its applicability, the proof of the existence and convergence of the solutions for different sets of problems one is referred to Mikhlin (1964) and Mikhlin and Smolitskiy (1967).

The other methods of integration such as the Fourier, Hankel and Laplace transform methods and the numerical method of Runge and Kutta will be described when they are applied in this thesis.

APPLICATION OF THE PERTURBATION METHOD TO THE STUDY OF THE DYNAMICS OF DEEP SEA CURRENTS IN COASTAL REGIONS IN THE NORTHEAST PACIFIC

Introduction to the Physical Problem and Derivation of Equations

Deep sea currents are poorly understood, complicated phenomena. They are composed of various types of steady state, transient and random components. Recent field observations obtained in the deep-sea region off the coast of California and Oregon (Isaacs et al., 1966; Nowroozi et al., 1968; Munk et al., 1970; and Korgen et al., 1970) indicate that the deep sea currents in the Northeast Pacific are mainly oscillating currents where the tidal components predominate. Hence in order to investigate analytically deep sea currents in this region the derivation of the tidal currents is of main interest. The first part of this thesis is devoted to this problem. The tidal currents in the Northeast Pacific will be computed in the long-wavelength approximation using a boundary perturbation method. A brief derivation of the basic equations follows below. The derivation of the tidal wave equations is presented here in a form close to the treatment by Fofonoff (1960) and Lamb (1932). For a more detailed description one is referred to these authors.

Consider a semi-infinite ocean in the f-plane (a plane where the Coriolis parameter $f = 2\Omega\sin\theta$, is assumed to be constant; Ω= angular

velocity of the earth's daily rotation, θ = geographic latitude). We will assume that g (the acceleration of gravity) is everywhere constant and vertically down. For simplification two kinds of notation, the Cartesian tensor notation and the x-y-z notation will be applied. The position is specified by a right-handed rectangular coordinate system (see Figure 1) with the origin at the mean free surface of the ocean, the x_1 or x-axis is directed northwards; x_2 or y-axis westwards and x_3 or z-axis upwards, parallel to the gravitational force. The velocity vectors will be denoted alternatively by (u_1, u_2, u_3) or (u, v, w).

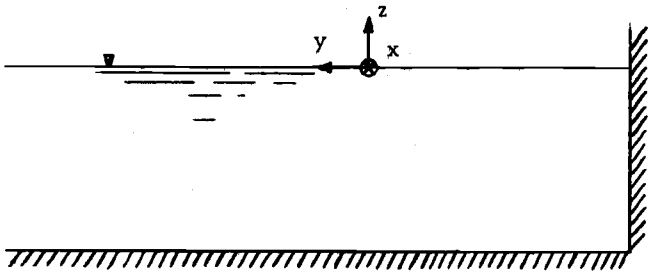

Figure 1. Basic coordinate system.

Using the tensor notation the Navier-Stokes equation is

$$\rho \frac{\partial u_i}{\partial t} + \rho u_j \frac{\partial u_i}{\partial x_j} + 2\rho \varepsilon_{ijk} \Omega_j u_k = - \frac{\partial p}{\partial x_i} - \rho g \delta_{3i} + \frac{\partial \sigma_{ij}}{\partial x_j} \qquad (7)$$

where ρ is the density; t the time; p the pressure; and Ω_i, the components of rotation at the earth's surface which are functions of x only. The σ_{ij}'s are the components of stress due to molecular viscosity. The symbol ε_{ijk} denotes the permutation tensor and δ_{ij} the Kronecker

delta. For a Newtonian fluid the stress tensor σ_{ij} is expressed as

$$\sigma_{ij} = \mu \left(\frac{\partial u_i}{\partial x_j} + \frac{\partial u_j}{\partial x_i} \right) \tag{8}$$

where μ is the molecular viscosity. The equation of conservation of mass is

$$\frac{\partial \rho}{\partial t} + \frac{\partial (\rho u_j)}{\partial x_j} = 0 \tag{9}$$

Substituting (8) and (9) into (7), the equation of conservation of momentum

$$\frac{\partial (\rho u_i)}{\partial t} + \frac{\partial (\rho u_i u_j)}{\partial x_j} + 2\rho \varepsilon_{ijk} \Omega_j u_k = -\frac{\partial p}{\partial x_i} - \rho g \delta_{3i} + \mu \frac{\partial^2 u_i}{\partial x_i \partial x_j} \tag{10}$$

is obtained. The equations (9) and (10) can be split into two sets of equations; one set represents the mean flow and the other the time-dependent flow, that is, the departure of the flow from its mean. These two sets of equations are not independent of each other, and each set contains terms representing interactions between the steady and time-dependent modes of motion. The separation of the flow is carried out by averaging equations (9) and (10) with respect to time. Let the time average of any property φ be defined as

$$\overline{\varphi} = \lim_{T \to \infty} \left(\frac{1}{2T} \int_{-T}^{T} \varphi \, dt \right) .$$

Moreover, we assume that

$$u_i = U_i + u_i'$$

$$p = P + p'$$

$$\rho = \overline{\rho} + \rho'$$

where U_i, P, $\overline{\rho}$ are the steady state parts and u_i', p', ρ' the time-dependent parts having zero averages. The assumption $\overline{\rho' u_i'} \ll \overline{u_i' u_j'}$ can be made because the variations of density in the ocean are of the order of 0.1% of the mean density, whereas velocity fluctuations are much larger and can be of the same magnitude as their mean. The equations for the steady state flow are

$$\overline{\rho} U_j \frac{\partial U_i}{\partial x_j} - \frac{\partial R_{ij}}{\partial x_j} + 2\varepsilon_{ijk} \Omega_j \overline{\rho} U_k = - \frac{\partial P}{\partial x_i} - \overline{\rho}\, g \delta_{3i} + \mu \frac{\partial^2 U_i}{\partial x_j \partial x_j} \quad , \tag{11}$$

$$\frac{\partial (\overline{\rho} U_j)}{\partial x_j} = 0 \quad , \tag{12}$$

where

$$R_{ij} = - \overline{\rho}\, \overline{u_i' u_j'}$$

is the Reynolds stress tensor. The equations of the time-dependent flow are

$$\overline{\rho} \frac{\partial u_i'}{\partial t} + \overline{\rho}\, U_j \frac{\partial u_i'}{\partial x_j} + \overline{\rho} u_j' \frac{\partial U_i}{\partial x_j} - \frac{\partial R'_{ij}}{\partial x_j} + 2\varepsilon_{ijk} \Omega_j \overline{\rho}\, u_k'$$

$$= - \frac{\partial p'}{\partial x_i} - \rho' g \delta_{3i} + \mu \frac{\partial^2 u_i'}{\partial x_j \partial x_j} \quad , \tag{13}$$

$$\frac{\partial p'}{\partial t} + \frac{\partial (\overline{\rho} u_j')}{\partial x_j} = 0 \, , \tag{14}$$

where

$$R'_{ij} = - \overline{\rho} \left(u_i' u_j' - \overline{u_i' u_j'} \right) .$$

In the following we will concentrate on the time-dependent equations (13) and (14).

In order to carry out an analysis of the order of magnitude of the various terms in equations (13) and (14), let L and H, be a characteristic length and depth, respectively, introduced to describe the horizontal and vertical scales of the motion. Moreover, let T_o, ρ_o, U_o, u_o, W_o, w_o, and f_o be characteristic values of t, ρ, U_i, u_i, W, w, and f respectively. Finally let $\Delta\rho_o$ indicate the characteristic density variations. The dimensionless forms of (13) and (14) can be derived

$$\frac{1}{f_o T_o} \frac{\partial u_i''}{\partial t'} + R_o \left[U_j' \frac{\partial u_i''}{\partial x_j'} + u_j'' \frac{\partial U_i'}{\partial x_j} - \left(\frac{u_o}{U_o} \right) \frac{\partial r_{ij}''}{\partial x_j'} \right] + \varepsilon_{ijk} \Omega_j' u_k''$$

$$= - \alpha' \frac{\partial p''}{\partial x_i'} + \frac{R_o}{R_e} \left[\nabla'^2 u_i'' + \left(\frac{L}{H} \right)^2 \frac{\partial^2 u_i''}{\partial x_3'^2} \right]$$

$$(i = 1, 2) \qquad (15)$$

$$F_r' \left(\frac{u_o}{U_o} \right) \left(\frac{H}{L} \right) \left[\frac{1}{(U_o/L)T_o} \frac{\partial u_3''}{\partial t'} + U_j' \frac{\partial u_3''}{\partial x_j'} + u_j'' \frac{\partial U_3'}{\partial x_j'} - \left(\frac{u_o}{U_o} \right) \frac{\partial r_{3j}''}{\partial x_j'} \right]$$

$$+ \frac{\rho_o u_o f_o}{\Delta\rho_o g} \varepsilon_{ijk} \Omega_j' u_k''$$

$$= - \frac{\partial p''}{\partial x_3'} - \rho'' + \frac{F_r'}{R_e} \left(\frac{u_o}{U_o} \right) \left(\frac{H}{L} \right) \left[\nabla'^2 u_3'' + \left(\frac{L}{H} \right)^2 \left(\frac{\partial^2 u_3''}{\partial x_3'^2} \right) \right] \qquad (16)$$

$$\frac{\Delta\rho_o}{\rho_o} \frac{1}{(U_o/L)T_o} \frac{\partial \rho''}{\partial t'} + \frac{\partial (\rho' u_j'')}{\partial x_j'} = 0 \qquad (17)$$

where the variables depending on time are denoted by double primes and

$$1/\rho' = \alpha' = \rho_o/\overline{\rho} \approx 1$$

$$r_{ij}'' = R_{ij}'/\rho_o u_o^2$$

$R_o = U_o/f_o L$, Rossby number

$R_e = \rho_o U_o L/\mu$, Reynolds number

$F_r' = U_o^2/(\Delta\rho_o/\rho_o)gH$, the internal Froude number.

It can thus be seen that the interaction terms (the interaction between the steady flow and the time-dependent flow) are important only when the Rossby number of the steady flow approaches unity. This can happen only for those comparatively concentrated currents such as the Gulf stream and Kuroshio. And the term containing r_{ij}'' will become important if the Rossby number for the time-dependent flow, $R_o u_o/U_o$, approaches unity. Just as in the steady state equations the terms representing molecular friction are negligible except for the case of extremely small scales of motion (this is dominated by R_o/R_e). In equation (16) F_r' can approach unity for ocean currents, but (H/L) is so small that the vertical acceleration can become appreciable only at very high frequencies. The vertical component of Coriolis force is also very small. Hence equation (16) can adequately be replaced by the hydrostatic equation.

Notice that by setting $U_i = 0$, ρ = constant and $\overline{u_i'u_j'} = 0$ in equations (13), (14), the general equations for the tides are obtained

(Hansen, 1960):

$$\left.\begin{aligned} &\frac{\partial u}{\partial t} + u\frac{\partial u}{\partial x} + v\frac{\partial u}{\partial y} - fv = -g\frac{\partial(\zeta - \bar{\zeta})}{\partial x} + S_x \\ &\frac{\partial v}{\partial t} + u\frac{\partial v}{\partial x} + v\frac{\partial v}{\partial y} + fu = -g\frac{\partial(\zeta - \bar{\zeta})}{\partial y} + S_y \\ &\frac{\partial \zeta}{\partial t} + \frac{\partial}{\partial x}[(h + \zeta)u] + \frac{\partial}{\partial y}[(h + \zeta)v] = 0 \end{aligned}\right\} \quad (18)$$

where ζ is the elevation of the tide above the mean sea surface $\bar{\zeta}$, S_x, S_y are the corresponding frictional terms and h is the ocean depth. The equation of continuity is obtained from the equation (14) by vertical integration. The velocity components u, v thus are barotropic, i.e., constants in any vertical line parallel to z.

Based on the order of magnitude analysis above and the additional assumption that the variation of ζ is small compared to that of mean depth h the following much simplified set of equations are obtained from equations (13) and (14) or (18):

$$\left.\begin{aligned} &\frac{\partial u}{\partial t} - fv = -g\frac{\partial(\zeta - \bar{\zeta})}{\partial x} \\ &\frac{\partial v}{\partial t} + fu = -g\frac{\partial(\zeta - \bar{\zeta})}{\partial y} \\ &\frac{\partial \zeta}{\partial t} + \frac{\partial(hu)}{\partial x} + \frac{\partial(hv)}{\partial y} = 0 \end{aligned}\right\} \quad (19)$$

These are the equations for the forced tidal waves in the long wave length approximation as described by Munk et al. (1970). Moreover the free long wave equations are obtained by setting $\bar{\zeta} = 0$ in equations (19):

$$\left.\begin{aligned} \frac{\partial u}{\partial t} - fv &= -g\frac{\partial \zeta}{\partial x} \\ \frac{\partial v}{\partial t} + fu &= -g\frac{\partial \zeta}{\partial y} \\ \frac{\partial \zeta}{\partial t} + \frac{\partial (hu)}{\partial x} + \frac{\partial (hv)}{\partial y} &= 0 \end{aligned}\right\} \quad (20)$$

Some theories and methods have been worked out to solve these equations. The most important method is the finite difference method, which reduces the problem to the solving of a set of algebraic difference equations (Hansen, 1960; Pekeris and Accad, 1969). This method has to be employed with care because of the uncertainties of the numerical stability (Collatz, 1960). As mentioned by Hansen (1960), "In any case the importance of each theory should be measured by the possibility of reproducing observed tides and currents in oceans and seas. The final problem of oceanic tides may be formulated as follows. The tides and tidal currents in the actual oceans have to be computed as a whole without using any tidal observations. For this computation only the well known tidal generating forces, the distributions of depth, and the shape of the coastal line along which the normal component of velocity is assumed zero are available. The efficiency of such a theory can be proved by means of tidal observations." This problem has to be solved completely and a tremendous amount of numerical work and analysis has to be carried out. Pekeris and Accad (1969) have made great advances in

this direction. In the case of the finite difference method the smaller the grid one uses, the more numerical calculation is involved and the more detailed knowledge of tides will be obtained. To reduce the amount of numerical work a small local area can be chosen. The accuracy of the calculations will then depend substantially on the accuracy of the boundary conditions, especially in the case of free boundaries, that is, boundaries which are not coastlines.

In the following the tidal currents in the coastal region of the northeast Pacific will be calculated on the basis of the long wave approximation given by equations (20). The applicability of this approximation has been discussed by a number of authors. It is of importance to note that for the case of California coastal waters, Larsen (1968) has shown that the magnitude and direction of the longshore phase velocity of M_2 tides along the coast is consistent with a simple Kelvin wave model (a type of free long wave solution of equations (20)) involving an ocean of a constant depth. He suggests that the amplitude of the M_2 component decreases offshore as a Kelvin wave. The abrupt change of depth profile in the shelf region and the effects of the borderland region off the southern California coast change the Kelvin wave amplitudes by only a few percent. Munk et al. (1970) come to similar conclusions. They attempt to interpret tidal observations along the California coast in terms of a superposition of three possible simple wave types, all of the same tidal

frequency: (a) a free Kelvin-like edge wave (the solution of the set of equations (20), mostly trapped by rotation, but somewhat slowed by the shelf); (b) a free Poincare-like leaky wave (another type of the solution of equations (20)); and (c) a forced wave where the distortion of the sea bottom by the tide plays a significant role. Their model can account for the main features of the observed tidal heights. On the other hand, tidal currents are not too accurately predicted by their model probably because of the problem associated with the separation of barotropic and baroclinic modes. Applying a step model (and a uniform depth model, too) for the continental shelf and slope off Depoe Bay, Oregon, Mooers (1970) discusses the various possibilities of the propagation of free or mixed Poincare and Kelvin types of waves in the region off the coast of Oregon.

Solution by Using the Boundary Perturbation Method

Introduction

As indicated above the approximate calculation of deep sea currents in the northeast Pacific coastal waters involves solving the basic equations for tidal currents in the linearized long wave approximation. A boundary perturbation method is employed to solve these equations when the bottom topography and coast line irregularities are considered. The interest centers on the computation of tidal

currents in the abyssal plain region off the coast of northern California, Oregon, and Washington, in particular, along the section from Cape Mendocino to Cape Flattery. The shore in this region is approximately a straight line, which simplifies the calculation.

As shown in the Figure 2 below, we consider a fluid-filled shallow semi-infinite basin of depth h(x, y).

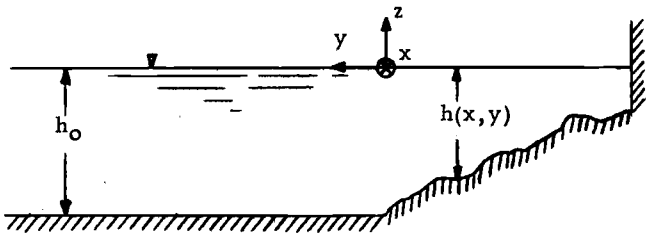

Figure 2. Cross section of the shallow semi-infinite model basin.

The coordinate axes and variables are as defined above. The equations (20) of the linearized long wave restated are

$$\left.\begin{aligned} \partial_t u - fv &= -g\,\partial_x \zeta \\ \partial_t v + fu &= -g\partial_y \zeta \\ \partial_x (uh) + \partial_y (vh) + \partial_t \zeta &= 0 \end{aligned}\right\} \quad (20)$$

Assuming a harmonic motion, that is ζ, u, v, $\propto \exp(i\omega t)$ and upon elimination of u and v this set of equations reduces to

$$(\nabla_2^2 + \frac{\omega^2 - f^2}{gh})\zeta + \frac{1}{h}\nabla h \cdot \nabla\zeta - \frac{f}{i\omega}\frac{1}{h}(\hat{z} \cdot \nabla h \times \nabla\zeta) = 0 \qquad (21)$$

where $\nabla_2^2 = \partial_{xx} + \partial_{yy}$ and $\hat{z}$ denotes a unit vector in the z-direction, with

$$u = \frac{-i\omega g}{\omega^2 - f^2}\left(\frac{\partial}{\partial x} - \frac{f}{i\omega}\frac{\partial}{\partial y}\right)\zeta$$

$$v = \frac{-i\omega g}{\omega^2 - f^2}\left(\frac{\partial}{\partial y} + \frac{f}{i\omega}\frac{\partial}{\partial x}\right)\zeta . \qquad (22)$$

For the solution of equation (21), appropriate boundary conditions (B.C.) have to be incorporated. Notice that since u and v are given by equations (22) it follows that u and v also satisfy equation (21). We will choose an appropriate straight line at sea level as the x-axis to separate the continental shelf and continental slope from the abyssal plain which can be assumed as an ocean of uniform depth h_0 (Figure 2).

The following section is devoted to the solution of the equation (21) with B.C. for $y > 0$. Before discussing details of the calculations, a short demonstration of the procedures to be involved is given below. We introduce the ocean models as shown in the following three diagrams.

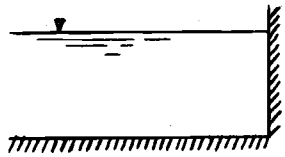

uniform ocean model

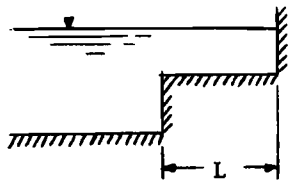

step shelf model

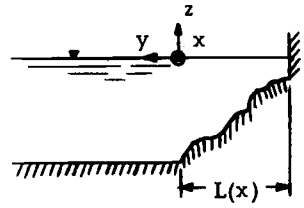

model with a real shelf profile

Using the boundary perturbation method to obtain approximate solutions for the real shelf profile model consists basically of three main steps.

(i) First the exact solutions of K, the wave number in the

x-direction, ζ, u and v are obtained for a step shelf model. Approximate solutions for this model are then derived by both

(a) the perturbation method to the first order, using the solutions of a uniform ocean model (Kelvin wave solutions) as the zeroth order approximations and

(b) the variational method.

Comparing the results under (a) and (b) with the exact solution, it is concluded that the perturbation method is more suitable.

Exact solutions of K, ζ, u and v are then obtained for the averaged cross section step shelf model for the region from Cape Mendocino to Cape Flattery, as shown in Figures 3, 4.

In this step equation (21) with the appropriate boundary conditions is solved for the step shelf models.

(ii) Using the above exact solution for the averaged step shelf model the component v at y = 0 is calculated for the real shelf profile model on the basis of the equation of continuity at y = 0. This equation is derived by calculating the flux of matter into the columnar space bounded by the rectangle $\delta x \delta y$ as shown in the following diagram;

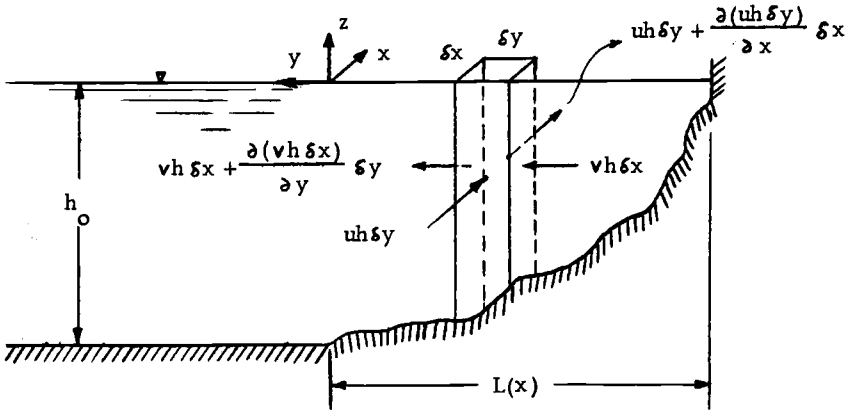

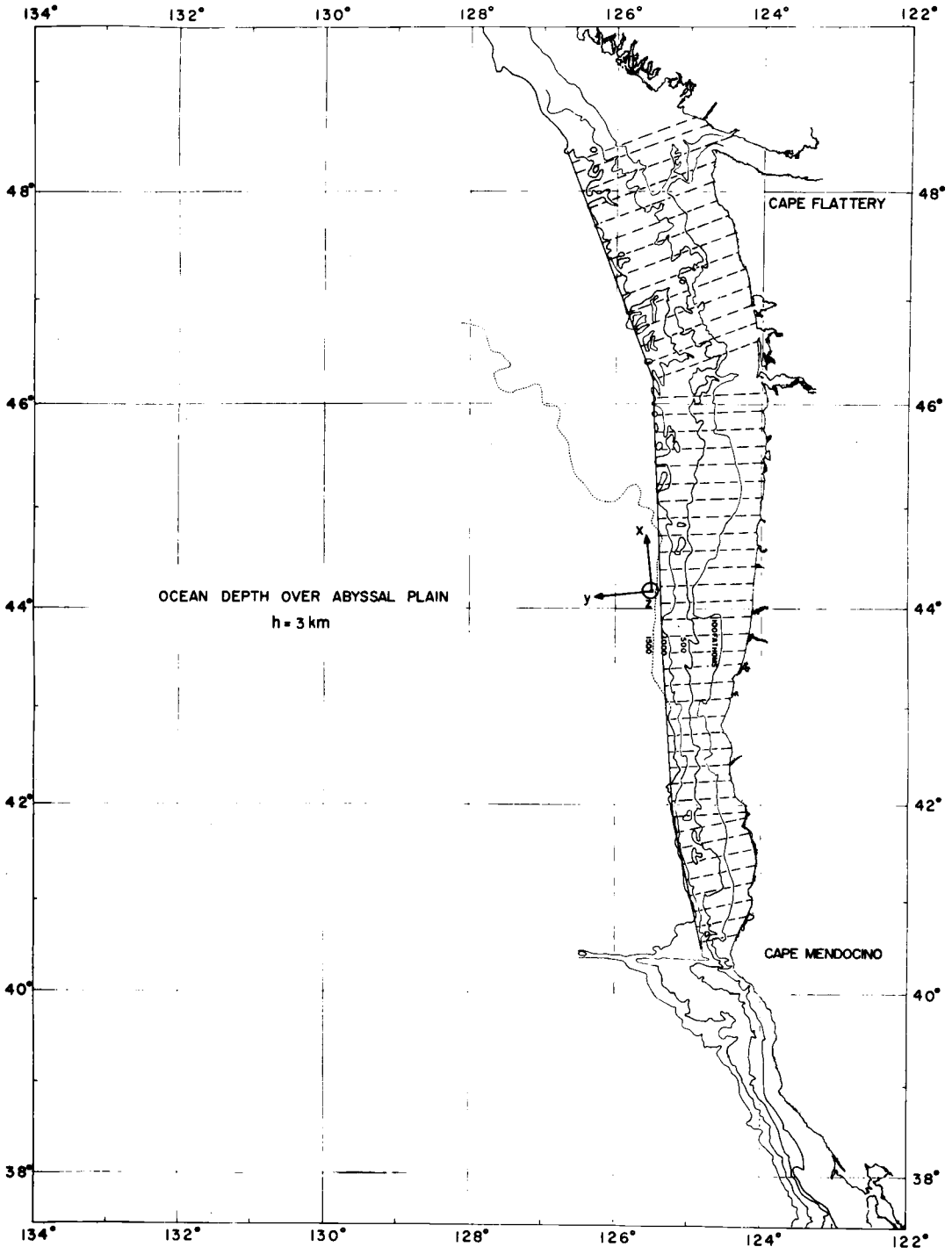

Figure 3. Generalized bathymetry contours from Cape Mendocino to Cape Flattery with the coordinate system used in the calculations. The dashed lines show where the cross sectional areas are calculated. The ocean depth over the abyssal plain is assumed to be 3 km.

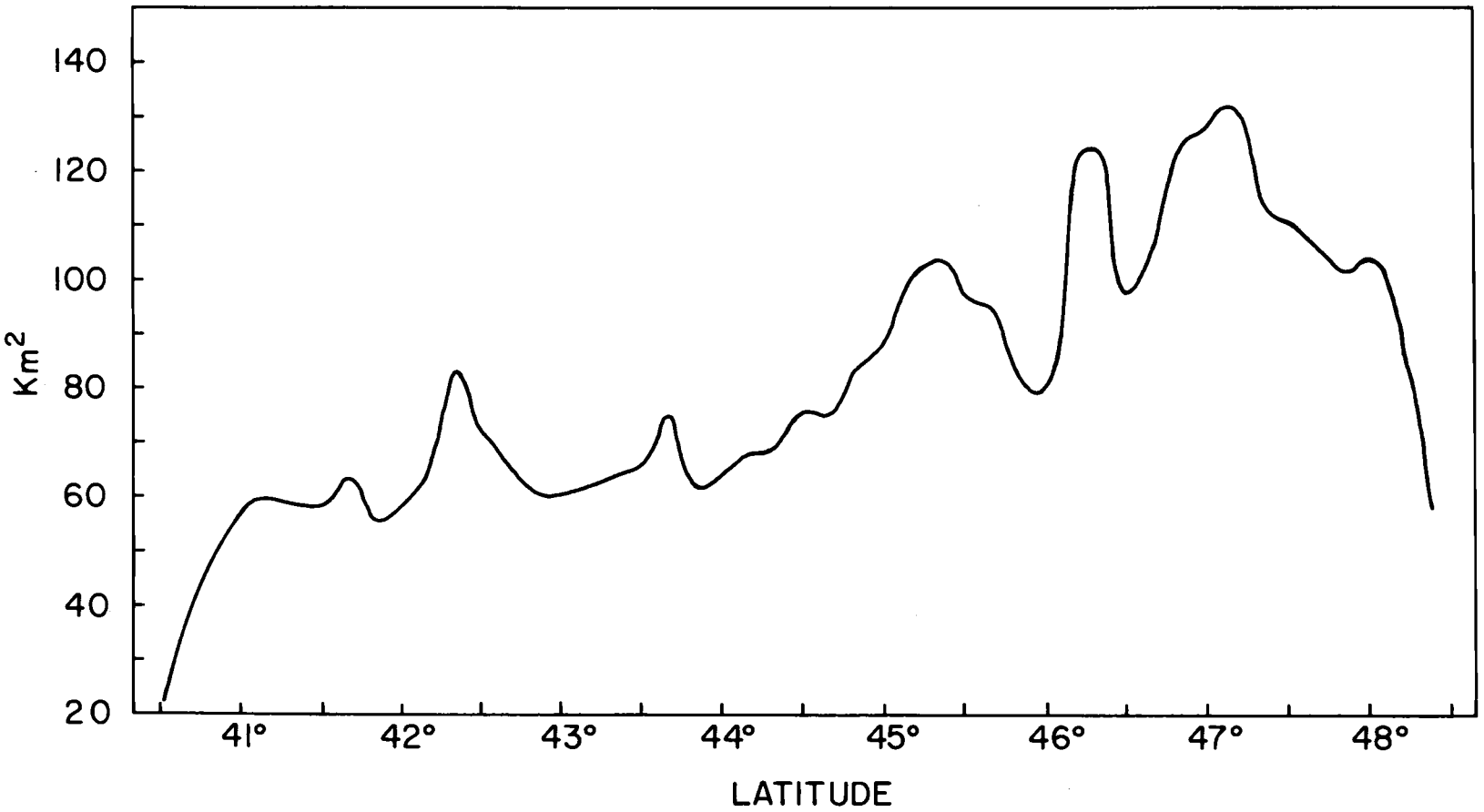

Figure 4. Cross sectional area curve from Cape Mendocino to Cape Flattery. The cross sectional area is calculated for each dashed line in Figure 3.

thus we have

$$\frac{\partial(uh\delta y)}{\partial x}\,\delta x + \frac{\partial(vh\delta x)}{\partial y}\delta y = -\frac{\partial}{\partial t}\{(\zeta + h)\,\delta x\delta y\}\ .$$

Since ζ, u, v and h are independent of y at y = 0, integration of the above equation in the y-direction yields

$$vh_o + \frac{\partial}{\partial x}(hLu) + L\frac{\partial \zeta}{\partial t} = 0\ ,$$

where L is the total width of the continental shelf and continental slope. Thus using the equation of continuity at y = 0 the perturbation solution, v_b, of v at the boundary y = 0 is expressed as

$$v_b = v_b^{(1)} + v_b'$$

where $|v_b'| \ll |v_b^{(1)}|$, $v_b^{(1)}$ is the exact solution of the averaged step shelf model and v_b', the perturbation correction.

(iii) The boundary values of v_b at y = 0 are used to solve the equation

$$(\nabla_2^2 + \frac{\omega^2 - f^2}{gh})\,v = 0 \qquad (23)$$

for y > 0 where $h = h_o$ (Figure 2). The Fast Fourier transform technique is used in the calculations in this step. Hence the perturbation solution of v for y > 0 is

$$v = v^{(1)} + v'$$

where $|v'| \ll |v^{(1)}|$, $v^{(1)}$ is the exact solution of the averaged step shelf model and v', the perturbation correction.

The three steps just mentioned will be described in detail as

follows.

Solution for the Averaged Step Shelf Model Case and Evaluation of the Method

Before the solution of the averaged step shelf case is derived, both the perturbation method and the variational method are used to solve equation (21) with B.C. for the step shelf model shown in the following diagram.

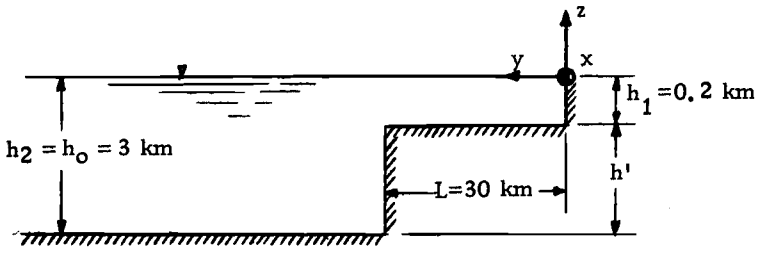

The M_2 tidal frequency (the period of the M_2 tidal component is 12.42 hour (Tomaschek, 1957)) is considered for the present case.

Although the exact solution cannot be obtained for the real shelf profile, it does exist for the step shelf case. It will be briefly derived as follows for the adopted model for the purpose of evaluation of the two approximate methods mentioned above. The equation to be solved is

$$(\nabla_2^2 + \frac{\omega^2 - f^2}{gh})\zeta = 0 \qquad (24)$$

with appropriate boundary conditions. Setting

$$\zeta = F(y)\exp[i(\omega t - Kx)] \quad \text{and} \quad y = YL$$

in (24) the following equation is obtained:

$$\frac{d^2F}{dY^2} + L^2 \left(\frac{\omega^2 - f^2}{gh} - K^2\right) F = 0 .$$

The solution is simply

$$F_1 = A \exp(m_1 Y) + B \exp(-m, Y) \quad \text{for } 0 \leq Y \leq 1$$

$$\text{where } m_1 = \sqrt{K^2 - \frac{\omega^2 - f^2}{gh}}\, L$$

$$F_2 = C \exp(-m_2 Y) \quad \text{for } 1 \leq Y < \infty \quad \text{where } m_2 = \sqrt{K^2 - \frac{\omega^2 - f^2}{gh}}\, L .$$

The following boundary conditions are to be satisfied:

$$\frac{\omega}{L}\frac{dF_1}{dY} + \omega f F_1 = 0 \quad \text{at } Y = 0$$

$$\left.\begin{aligned} F_1(1) &= F_2(1) \\ h_1\left(\frac{\omega}{L}\frac{dF_1}{dY} + \omega f F_1\right) &= h_2\left(\frac{\omega}{L}\frac{dF_2}{dY} + \omega f F_2\right) \end{aligned}\right\} \text{ at } Y = 1 .$$

The dispersion relation is then

$$\frac{h_1}{h_2}\left[\left(\frac{m_1}{L}\right)^2 - \left(\frac{fK}{\omega}\right)^2\right] + \left(\frac{m_2}{L} - \frac{fK}{\omega}\right)\left[\frac{m_1}{L}\,\text{cothm}_1 - \frac{fK}{\omega}\right] = 0 . \qquad (25)$$

From this relation we obtain that $K = 8.3377 \times 10^{-4}\,km^{-1}$ and the corresponding solutions are consequently

$$F_1 = \cos(0.05997Y) - 0.3048 \sin(0.05997Y)$$

$$F_2 = 0.988278 \exp(-0.01851Y),$$

requiring that $\zeta = 1$ at $Y = 0$. Finally the solutions of interest to us for ζ, u, v, can be calculated as follows (refer to p. 19):

$$\zeta = F(y)\ \exp[i(\omega t - Kx)]$$

$$u = \frac{-i\omega g}{\omega^2 - f^2}\left(\frac{\partial}{\partial x} - \frac{f}{i\omega}\frac{\partial}{\partial y}\right)\zeta$$

$$v = \frac{-i\omega g}{\omega^2 - f^2}\left(\frac{\partial}{\partial y} + \frac{f}{i\omega}\frac{\partial}{\partial x}\right)\zeta \quad . \qquad (22)$$

(a) Solution by the perturbation method. The above problem will now be solved by the perturbation method. Assuming that

$$\zeta = F(y)\ \exp[i(\omega t - Kx)]$$

we obtain from equation (21) the following equation for F(y):

$$\frac{d}{dy}\left(h\frac{dF}{dy}\right) + \left(\frac{\omega^2 - f^2}{g} + \frac{fK}{\omega}\frac{dh}{dy} - K^2 h\right)F = 0 \qquad (26)$$

with boundary conditions

$$\omega\frac{dF}{dy} + KfF = 0 \quad \text{at } y = 0$$

$$F = 0 \quad \text{as } y \to \infty \quad .$$

Making the transformation $y = LY$ equation (26) becomes

$$h\frac{d^2F}{dY^2} + L^2\left(\frac{\omega^2 - f^2}{g} - K^2 h\right)F + \frac{dh}{dY}\frac{dF}{dY} + \frac{fK}{\omega}L\frac{dh}{dY}F = 0 \qquad (27)$$

with boundary conditions

$$F = 0 \text{ as } Y \to \infty$$

$$\frac{\omega}{L}\frac{dF}{dY} + KfF = 0 \text{ at } Y = 0.$$

For the first order solutions we let

$$
\begin{aligned}
F &= F_o + F' \\
K &= K_o + K' \\
h &= h_o + H \\
H &= -h' + h' \mathbb{1}(Y - 1)
\end{aligned}
\tag{28}
$$

where $\mathbb{1}$ is the unit step function, and we assume that $|F'| << |F_o|$, $|K'| << |K_o|$ and $H << h_o$. Inserting (28) into (27) and neglecting the second order terms the following equation is arrived at:

$$h_o \frac{d^2F'}{dY^2} + L^2\left(\frac{\omega^2 - f^2}{g} - K_o{}^2 h_o\right)F' = \mathcal{R}.$$

where

$$\mathcal{R} = L^2(K_o{}^2 h' + 2K_o K' h_o)F_o - h'\frac{d^2F_o}{dY^2} - \frac{dh'}{dY}\frac{dF_o}{dY} - \frac{fK}{\omega} L \frac{dh'}{dY} F_o ,$$

and F_o is a zeroth order Kelvin wave solution for a uniform semi-infinite basin of depth h_o. This solution is derived from equation (24):

$$(\nabla_2^2 + \frac{\omega^2 - f^2}{gh})\,\zeta = 0$$

or

$$h_o \frac{d^2F_o}{dY^2} + L^2\left(\frac{\omega^2 - f^2}{g} - K_o{}^2 h_o\right)F_o = 0$$

with the boundary conditions

$$F_o = 0 \qquad \text{as } Y \to \infty$$

$$\frac{\omega}{L}\frac{dF_o}{dY} + K_o f F_o = 0 \quad \text{at } Y = 0 ;$$

just like the equations solved in the step shelf case above. The

solutions can simply be written as follows:

$$\left.\begin{aligned} K_o &= \frac{\omega}{\sqrt{gh_o}} \\ F_o &= \text{constant} \times \exp\left[- \frac{f}{\sqrt{gh_o}} LY \right] \\ \zeta &= F_o \exp[i(\omega t - Kx)] \\ u &= \frac{gK_o}{\omega} \\ v &= 0 \quad . \end{aligned}\right\} \quad (29)$$

Since for the problem at hand the operator $\mathcal{M}$,

$$\mathcal{M} = h_o \frac{d^2}{dY^2} + L^2 \left(\frac{\omega^2 - f^2}{g} - K_o{}^2 h_o \right),$$

is hermitian (which can easily by shown) it is required that

(Courant and Hilbert, 1953)

$$(\mathcal{R}, F_o) = \int_0^\infty \mathcal{R} F_o \, dY = 0 \quad .$$

We find the $K' = 0.13523 \times 10^{-4} \text{ km}^{-1}$ and consequently

$K = 8.33084 \times 10^{-4} \text{ km}^{-1}$.

In order to obtain F' we have to derive the Green function G of the operator $\mathcal{M}$. This G can be found from the solutions of the equation

$$h_o \frac{d^2 G}{dY^2} + L^2 \left(\frac{\omega^2 - f^2}{g} - K_o{}^2 h_o \right) G = \delta (Y - Y') \, .$$

As shown in the diagram below

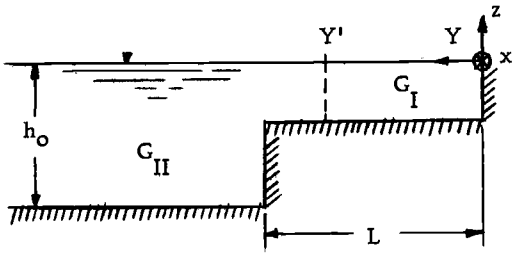

the boundary conditions required are

$$G_{II} = 0 \text{ as } Y \to \infty ,$$

$$\frac{\omega}{L}\frac{dG_I}{dY} + K_o f G_I = 0 \text{ at } Y = 0$$

and that G and dG/dY are continuous at $Y = Y'$. The Green function is

$$G_I = \frac{\exp(-m_1 Y')}{2 m_1 h_o} \exp(m_1 Y) + \frac{\frac{\omega}{L} m_1 + K_o f}{\frac{\omega}{L} m_1 - K_o f} \frac{\exp(-m_1 Y')}{2 m_1 h_o} \exp(-m_1 Y)$$

$$G_{II} = \left(\frac{\exp(m_1 Y')}{2 m_1 h_o} + \frac{\frac{\omega}{L} m_1 + K_o f}{\frac{\omega}{L} m_1 - K_o f} \frac{\exp(-m_1 Y')}{2 m_1 h_o} \right) \exp(-m_1 Y) ,$$

and F' is derived from R * G, the convolution of R and G. The functions of ζ, u and v are consequently obtained (using equations (22)).

(b) Solution by a variational method.

We write (27) in the form represented by an operator $\mathcal{A}$ such that

$$\mathcal{A} F = 0 \tag{30}$$

where

$$\mathcal{A} = h \frac{d^2}{dY^2} + L^2 \left(\frac{\omega^2 - f^2}{g} - K^2 h \right) + \frac{dh}{dY} \frac{d}{dY} + \frac{fK}{\omega} L \frac{dh}{dY} .$$

We choose the coordinate function to be

$$\mathcal{L}_n(Y) = \sqrt{2b}\, \exp(-bY)\, \frac{L_n(2bY)}{n!} \quad ,$$

where

$$L_n(Y) = n! \sum_{m=0}^{n} \binom{n}{n-m} \frac{(-Y)^m}{m!}$$

are the Laguerre polynomials (Morse and Feshbach, 1953; Erdélyi et al., 1953). The coordinate function satisfies the boundary condition as $Y \to \infty$, and

$$\int_0^\infty \mathcal{L}_n \mathcal{L}_m \, dY = \delta_{nm} \quad ,$$

which simplifies our later calculation of the matrix elements. We form the approximate solution to (30) as

$$F = \sum_i a_i \mathcal{L}_i(Y) + c \exp(-b'Y)$$

where a_i and c are arbitrary constants to be determined. In this calculation we assume b = 0.01851, which is equal to the constant m_2 obtained for the exact solution F_2 (see p. 25). The constant b' is estimated by trial and error at 7.26×10^{-4} by carrying out the orthogonal expansion of the exact solution F into a series of $\mathcal{L}_n$. The constants a_i and c are calculated by

$$\left.\begin{aligned} (AF, \mathcal{L}_i) &= 0 \text{ for all } i \\ (AF, \exp(-b'Y)) &= 0 \end{aligned}\right\} \quad (31)$$

and the boundary condition

$$-\omega \frac{dF}{dY} + L\, f\, K\, F = 0 \text{ at } Y = 0 \, ,$$

requiring that $\zeta = 1$ at $Y = 0$. Recognizing that this is an eigenvalue problem, and setting the determinant obtained from equations (31) equal to zero the approximate wave number K can be found. From this K value the constants a_i, c can then be calculated. If we let $i = 6$ the matrix formulated from equations (31) is:

(see p. 32)

For $i = 3$ the solution of K is approximately $9.59 \times 10^{-4} Km^{-1}$, which is greater than the exact value, and the constants a_i, c are

$$a_o = -3.5265 \times 10^{-4}$$

$$a_1 = 1.34413 \times 10^{-4}$$

$$a_2 = -2.664 \times 10^{-5}$$

$$c = 1.00098.$$

The K value obtained for the $i = 2$ case is less than the exact value. This suggests that the approximate K values oscillate around the exact value. It can be seen easily that higher values of i yield better approximations; however, the amount of numerical work will at the same time become very large for both the evaluation of the matrix elements and the expansion constants.

Following a comparison of the results from both the perturbation and the variational methods it is concluded that for the problem at hand the perturbation method is to be preferred.

Referring to Figure 3 the cross sectional areas of the continental shelf waters are calculated for lines perpendicular to the approximate

$$
\begin{bmatrix}
64.00419-900K^2 & 256 & 512 & 768 & 1024 & 1280 & 2.25\times10^{-3}-448.99K^2 \\
7\times10^{-9} & 64.00419-900K^2 & 256 & 512 & 768 & 1024 & -2.23\times10^{-3}+446.97K^2 \\
-4.9\times10^{-8} & 7.9\times10^{-7} & 64.00419-900K^2 & 256 & 512 & 768 & 2.15\times10^{-3}-444.96K^2 \\
1.9\times10^{-7} & -3.2\times10^{-6} & 2.3\times10^{-5} & 64.00410-900K^2 & 256 & 512 & -1.86\times10^{-3}+442.96K^2 \\
-4.6\times10^{-7} & 7.6\times10^{-6} & -5.5\times10^{-5} & 2.3\times10^{-4} & 64.00361-900K^2 & 256 & 1.17\times10^{-3}-440.97K^2 \\
6.2\times10^{-7} & -1.0\times10^{-5} & 7.7\times10^{-5} & -3.3\times10^{-4} & 8.8\times10^{-4} & 64.00273-900K^2 & -0.25\times10^{-3}+438.98K^2 \\
32-88.3K & 96-88.3K & 160-88.3K & 224-88.3K & 288-88.3K & 352-88.3K & 0.01803-22.08K
\end{bmatrix}
$$

boundary between the continental slope and the abyssal plain. The contours from bathymetric maps[1] have been digitized for the calculation of cross sectional areas using the CDC 3300 computer at Oregon State University. The results are plotted as shown in Figure 4. These cross sectional areas are averaged algebraically and the lengths of the lines perpendicular to the boundaries of the continental slope and the abyssal plain are also averaged. From these results the averaged step shelf model for the area of interest from Cape Mendocino to Cape Flattery is obtained as shown in Figure 5:

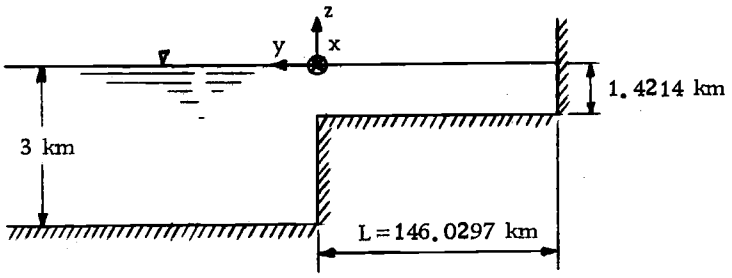

Figure 5. The averaged step shelf model for the area from Cape Mendocino to Cape Flattery.

The exact solutions for K, ζ, u_{av}, and v_{av} of this averaged step shelf model can be obtained just like those derived on p. 25.

---

[1] C.&G.S. 1308-12 (1969), C.&G.S. 1308 N-17 (1968), C.&G.S. 1308 N-22 (1968) published at Washington, D.C., U.S. Department of Commerce, National Oceanic and Atmospheric Administration, National Ocean Survey; and C.&G.S. 5022 (1971), C.&G.S. 5052 (1971), C.&G.S. 6002 (1971), C.&G.S. 6102 (1973) published at Washington, D.C., U.S. Department of Commerce, Environmental Science Services Administration, Coast and Geodetic Survey.

Assuming a tidal height ζ at y = 0 of 1 meter the results are presented in the following table as compared to the corresponding Kelvin wave solutions of a semi-infinite uniform ocean basin of a depth 3 km. The frequency of the M_2 tidal component is being used and the velocity components u_{av} and v_{av} are calculated at y = 0.

Table 1. Solutions of K, $|u_{av}|$, $|v_{av}|$ of the averaged step shelf model compared with those of the Kelvin wave solutions.

the solution / specific model	K (wave number) km^{-1}	$\|u_{av}\|$ at y = 0 cm/sec	$\|v_{av}\|$ at y = 0 cm/sec
averaged step shelf model	8.5901×10^{-4}	5.717	0.3444
Kelvin wave uniform depth model	8.1956×10^{-4}	5.7155	0

The exact solutions for K, ζ, u_{av}, and v_{av} for the averaged step shelf model have also been calculated for the frequency of the K_1 tidal component (the period of the K_1 tidal component is 23.93 hour (Tomaschek, 1957)), which shows a K value of 4.2538×10^{-4} km^{-1} and v_{av} = -0.17994 cm/sec at y = 0.

Boundary Condition at y = 0

The averaged step shelf model is shown in the diagram below.

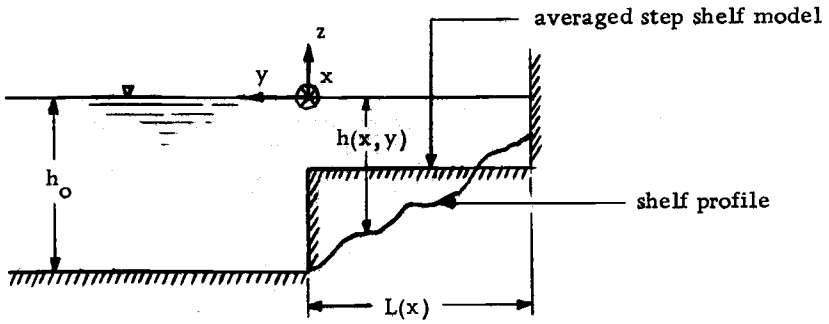

Let L(x) be the width of the continental shelf and the continental slope, which varies along the x-axis. The continuity equation at y = 0 as derived before (p. 23) is

$$v h_o + \frac{\partial}{\partial x} (h L u) + L \frac{\partial \zeta}{\partial t} = 0 \quad . \tag{32}$$

To obtain a wave number value K we insert the averaged values of (Lh) and L, which are derived from the averaged step shelf model (refer to the diagram of p. 33), into this equation and use the exact formulae for ζ, u, and v calculated for a step shelf model (refer to p. 26) with $y > 0$ assuming $\zeta = 1$ at $y = 0$:

$$\left.\begin{aligned} \zeta &= \exp\left(- \sqrt{K^2 - \frac{\omega^2 - f^2}{g h_o}}\, y \right) \exp\left[i(\omega t - Kx) \right] \\ u_{av} &= \frac{g}{\omega^2 - f^2} \exp\left[i(\omega t - Kx) \right] \left(f \frac{d}{dY} + \omega K \right) \exp\left(- \sqrt{K^2 - \frac{\omega^2 - f^2}{g h_o}}\, y \right) \\ v_{av} &= \frac{ig}{\omega^2 - f^2} \exp\left[i(\omega t - Kx) \right] \left(\omega \frac{d}{dY} + Kf \right) \exp\left(- \sqrt{K^2 - \frac{\omega^2 - f^2}{g h_o}}\, y \right) \end{aligned}\right\} \tag{33}$$

(Notice that equations (33) are just the rewritten results stated in

p. 26). This value is the same as already obtained in the last section by the dispersion relation (see p. 25, p. 34). The corresponding result of u_{av} at y = 0 is thus also the same as it is stated in p. 34. The v_{av} value can be calculated in two ways, either from equation (32) by inserting the known values of K and u or by using equations (33) directly. The results are identical. The second way stated is the same as that used in p. 33. These results are the exact solutions for the averaged step shelf model. Taking into consideration the real shape of the continental shelf, the continental slope and the coast line (h and L vary in the x-y plane), the approximate values of v at the boundary y = 0 can be calculated by using equation (32) and the exact solutions of K, ζ and u for the averaged step shelf model. Substituting equation (33) into the equation of continuity at y = 0, (32), letting u = u_{av}, the approximation for v at y = 0 is obtained

$$v = \frac{1}{h_o}\{\frac{g}{\omega^2 - f^2}(-f\sqrt{K^2 - \frac{\omega^2 - f^2}{gh_o}} + \omega K)[ih(x,y)L(x)K - \frac{\partial}{\partial x}(h(x,y)L(x)] - i\omega L(x)\}$$

$$x \exp[i(\omega t - Kx)] \quad . \qquad (34)$$

These results are used in the next step for the computation of v for y > 0. This process can be repeated and further approximations for K, u and v can thus be obtained.

Solution

We assume that

$$v = v^{(1)} + v' \ , \quad \text{where } |v'| << |v^{(1)}|$$

and at $y = 0$

$$v = v_b = v_b^{(1)} + v_b' \ , \quad \text{where } |v_b'| << |v_b^{(1)}| \ .$$

$v^{(1)}$ and $v_b^{(1)}$ are the exact solutions for the averaged step shelf model, which have been obtained previously (pp. 31-34). Moreover v_b has been obtained in the last section (pp. 34-36). The perturbation correction, v_b', is now used for the computation of v' for $y > 0$. The equation

$$\frac{\partial^2 v'}{\partial x^2} + \frac{\partial^2 v'}{\partial y^2} + \frac{\omega^2 - f^2}{gh_o} v' = 0 \qquad (35)$$

with the boundary condition

$$v' = v_b' \text{ at } y = 0$$

is to be solved. Referring to the diagram below,

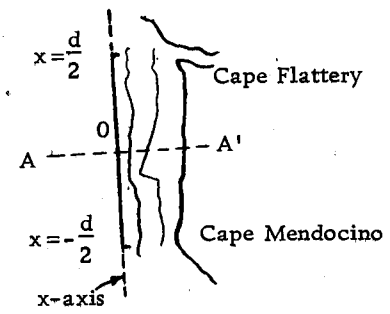

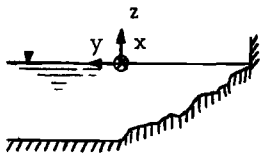

The cross section at AA'.

we assume that $h(x, y)$ and $L(x)$ vary only in the region between $x = -\frac{d}{2}$ and $x = \frac{d}{2}$. Outside $x - [-\frac{d}{2}, \frac{d}{2}]$ the solution for v is $v^{(1)}$ for $y \geq 0$ obtained in the two previous sections. The Fourier transform of equation (35) yields

$$\frac{d^2\hat{v}'(\ ,y)}{dy^2} + \left(\frac{\omega^2 - f^2}{gh_o} - s^2\right)\hat{v}'(s,y) = 0 \qquad (36)$$

where

$$\hat{v}'(s,y) = \frac{1}{\sqrt{2\pi}}\int_{-\infty}^{\infty} v'(x,y)\exp(-isx)\,dx \quad .$$

The solution of equation (36) is

$$\hat{v}' = \hat{v}_b'\exp\left[-\sqrt{s^2 - \frac{\omega^2 - f^2}{gh_o}}\,y\right] \qquad (37)$$

requiring that $\hat{v}'$ goes to zero as $y \to \infty$. The v_b' is the Fourier transform of v_b'. The inverse Fourier transform of equation (37) would then give the solution of v'. The Fourier transform pair is carried out here by using the programs stored in OS-3 ARAND SYSTEM at Oregon State University, written by Ochs et al. (1970) and Ballance et al. (1971) employing the Fast Fourier Transform technique (Cooley and Tukey, 1965; Cooley et al., 1967). These programs for the Fourier transform pair can be represented by the following two equations:

$$B(n) = \sum_{t=0}^{N-1} A(t)\exp\left[-\frac{i2n\pi t}{N}\right]$$

$$A(t) = \frac{1}{N}\sum_{n=0}^{N-1} B(n)\exp\left[\frac{i2n\pi t}{N}\right] \quad .$$

They are finite discrete Fourier transforms where N is the total number of points, which has to be a number of the integer power of 2. The functions A and B are sampled at these points which are represented by n and t. It is noticed that this Fourier transform pair is

not symmetric. The cross sectional area curve (Figure 4) is sampled at 64 points in equal space. The approximate values of v at y = 0 along the x-axis are then calculated at these 64 points using the method described in the last section. After the subtractions of v_{av} (at y = 0) from these values at all the specific points, the result is

$$v_b'(t), \quad t = 1, 2, \ldots 64 ;$$

which are complex variables. The Fourier transform of them is carried out by the programs stated above:

$$\hat{v}_b'(n) = \sum_{t=0}^{N-1} v_b'(t) \exp\left[- \frac{i2n\pi t}{N} \right] \tag{38}$$

where N = 64. It is to be noted that the infinite Fourier transform has been replaced by the finite Fourier transform

$$\hat{v}_b'(s) = \int_{-\infty}^{\infty} v_b'(x) \exp(-isx)\, dx = \int_{-\frac{d}{2}}^{\frac{d}{2}} v_b'(x) \exp(-isx)\, dx .$$

Equation (38) is obtained by writing $s = \frac{2n\pi}{d}$. Substituting (38) into equation (37) and carrying out the inverse Fourier transform we get

$$v'(t, y) = \frac{1}{N} \sum_{n=0}^{N-1} \left(\sum_{t=0}^{N-1} v_b'(t) \exp\left[- \frac{i2n\pi t}{N} \right] \right) \exp\left[- \sqrt{\left(\frac{2n\pi}{d}\right)^2 - \frac{\omega^2 - f^2}{gh_o}}\, y \right] \exp\left(i \frac{2n\pi t}{N}\right).$$

The final approximate values of v(x, y) are obtained for y > 0 on the basis of

$$v(x,y) = v^{(0)}(x, y) + v'(x, y) .$$

The data has been calculated for both the semi-diurnal (M_2) tidal frequency and the diurnal (K_1) tidal frequency. The results are

presented in Figure 6 and Figure 7. The amplitude of the sea surface elevation at the boundary $y = 0$, $\zeta(x, 0)$ has been normalized to 1 meter.

Conclusion

Above we have demonstrated the application of the perturbation method to the computation of deep sea currents in coastal regions of the northeast Pacific. The principal reason to resort to this method is the rather irregular shape of the coastal contours in the region, which prevents the derivation of exact solutions. The example presented illustrates quite well the advantages of the method in this case. The application is quite straightforward and presents no major problems. The results furnish a detailed picture of the deep sea currents which can be expected in the region.

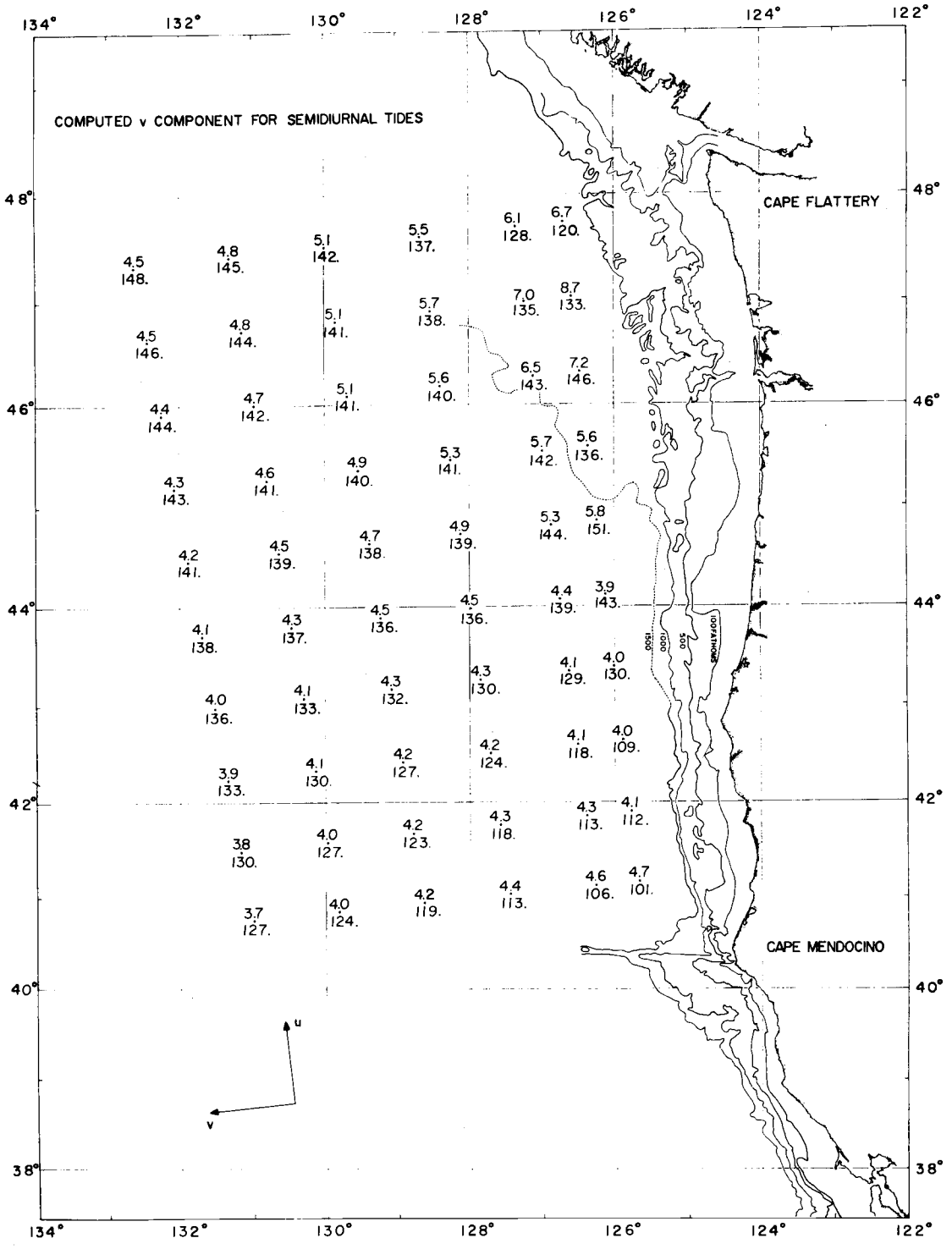

Figure 6. Computed v component for semi-diurnal tides when the amplitude of the surface elevation at the boundary, $\zeta(x,0)$, has been normalized to 1 meter. At each station, the upper number gives the amplitude of v in mm/sec and the lower number gives the phase-lag in degrees relative to the surface elevation ζ.

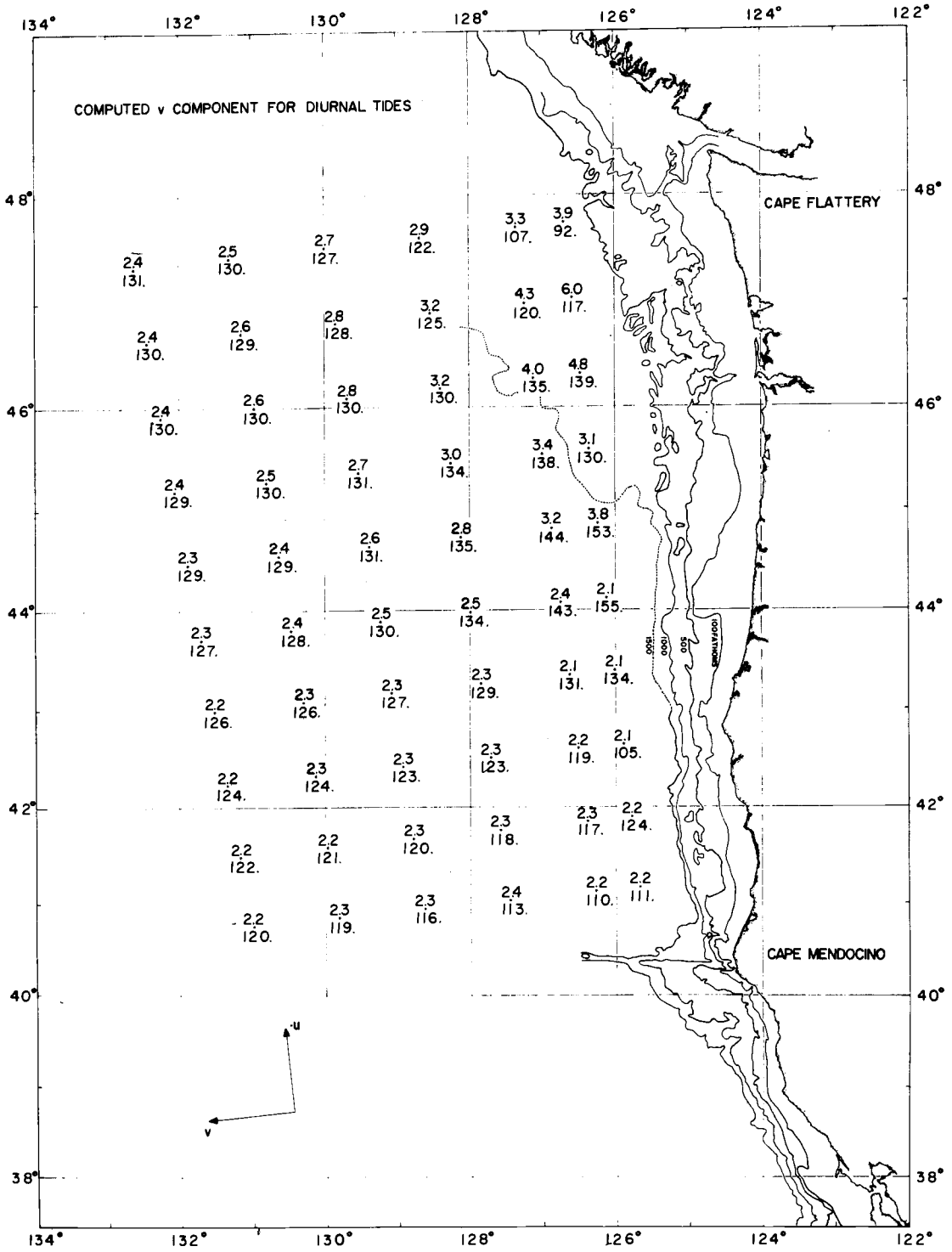

Figure 7. Computed v component for diurnal tides when the amplitude of the surface elevation at the boundary, $\zeta(x,0)$, has been normalized to 1 meter. At each station, the upper number gives the amplitude of v in mm/sec and the lower number gives the phase-lag in degrees relative to the surface elevation ζ.

APPLICATION OF THE PERTURBATION TECHNIQUE TO THE INTERPRETATION OF D. C. CONDUCTION DATA IN EXPLORATION GEOPHYSICS

Introduction to the Physical Problem and Derivation of Equations

There are in general two types of methods for the interpretation of D. C. conduction data, the direct method and the indirect method. The indirect method involves comparing the observed apparent resistivity data with a set of theoretical curves calculated for certain specific models (Compagnie Generale de Geophysique, La., 1955; Mooney and Wetzel, 1956). Undoubtedly, this method, though convenient to use, has severe limitations. The limited number of theoretical curves makes it impossible to fully extract all the information contained in the data. Also the problem of uniqueness is always raised. The difficulties of the indirect approach may in many cases be partially overcome by using the direct method of interpretation. Langer (1933) has shown that if the conductivity of the ground is a function of depth only then the potential around a point current electrode uniquely determines this function. A direct computation of the conductivity from the observed data is therefore in principle possible. One of the first direct methods was proposed by Slichter (1933). Later contributions have been made by Pekeris (1940), Vozoff (1956), Koefoed (1965 and 1966), Paul (1968), Fritsch and Zschau (1969),

Chan (1970). Generally speaking, two main steps are involved: (1) from the apparent resistivity data a function, known as the kernal (Slichter kernel, Slichter, 1933; Stefanesco kernel, Stefanesco and Schlumberger, 1930), is calculated then (2) the continuous resistivity function of the earth (or layer resistivities and thicknesses of a stratified earth model) is determined on the basis of the resulting kernel. In this process, an integral equation relating the true resistivity and the observational data is solved by the iteration method. A considerable amount of numerical work is involved in this process. A completely different approach has been developed by Kunetz and Rocroi (1970). They start from a different integral representation of the apparent resistivity containing the modified Bessel function in place of the Bessel function. The least square method is used in their approach for the solution of the integral equation, and the possibility of obtaining physically unacceptable results (e.g. negative thicknesses and resistivities) is excluded by their technique. Lee (1972) proposed a direct method for the interpretation of resistivity data over a more complex two dimensional resistivity structure where the surface of discontinuity of the resistivity is a curved surface. Apparently in all these direct methods, the first approximation of the geological structure and its resistivity is very important to the success of the application of the particular method. This thesis provides an alternative approach to the indirect and direct methods in the interpretation

of a certain class of resistivity data by using a perturbation technique.

The basic equations for the electrical conduction method are as follows. Let $\vec{H}$ be the magnetic intensity, $\vec{J}$ the current density, $\vec{J}_s$ the source current density, $\vec{E}$ the electric field, and V the electric scalar potential; all measured in MKS units. From the time-independent Maxwell's equations

$$\nabla \times \vec{H} = \vec{J} + \vec{J}_s$$

$$\nabla \times \vec{E} = 0$$

and Ohm's law

$$\vec{J} = \sigma \vec{E} ,$$

where σ is the electric conductivity, the following equation is obtained:

$$\nabla \cdot (-\sigma \nabla V + \vec{J}_s) = 0 . \qquad (39)$$

Equation (39) can be written as

$$\nabla \cdot (\sigma \nabla V) = S , \qquad (40)$$

where $S = \nabla \cdot \vec{J}_s$ is the source density.

Solution to the Problem in General

(i) General Solution

If S is a concentrated or point source located at the surface of the ground, σ is a function of depth z only, and I is the input current (refer to the diagram below),

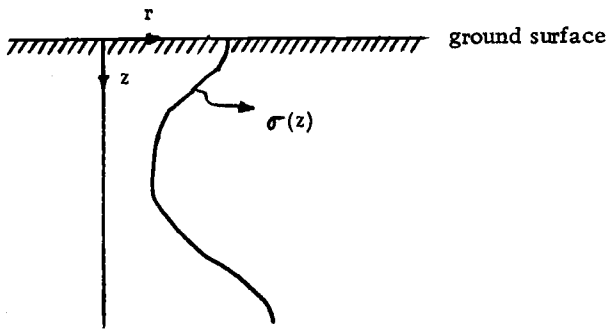

equation (40) written in cylindrical coordinates (r, θ, z) reduces to

$$\frac{\partial^2 V}{\partial r^2} + \frac{1}{r}\frac{\partial V}{\partial r} + \frac{1}{\sigma(z)}\frac{\partial}{\partial z}\left(\sigma(z)\frac{\partial V}{\partial z}\right) = -\frac{I}{\sigma_s}\frac{\delta(r)\delta(z)}{2\pi r} \quad , \tag{41}$$

where σ_s is the electric conductivity at the surface of the ground $z = 0$. The other boundary condition is that $V = 0$ as $z \to \infty$. The Hankel transform of $V(r, z)$ is defined as

$$\hat{V}(k, z) = \int_0^\infty V(r, z) J_o(kr) r \, dr \quad , \tag{42}$$

where $J_o(kr)$ is the Bessel Function of the first kind of order zero. Applying the transform to equation (41) results in

$$\frac{d^2\hat{V}}{dz^2} + \frac{1}{\sigma(z)}\frac{d\sigma(z)}{dz}\frac{d\hat{V}}{dz} - k^2\hat{V} = -\frac{I\delta(z)}{2\pi\sigma_s} \quad .$$

The boundary condition now becomes $\hat{V} = 0$ as $z \to \infty$. This equation can be replaced by the following equation:

$$\frac{d^2\hat{V}}{dz^2} + \frac{1}{\sigma(z)}\frac{d\sigma(z)}{dz}\frac{d\hat{V}}{dz} - k^2\hat{V} = 0 \quad , \tag{43}$$

with the boundary conditions

$$\frac{d\hat{V}}{dz} = -\frac{I}{2\pi\sigma_s} \quad \text{at } z = 0 \text{ and } \hat{V} = 0 \text{ as } z \to \infty. \tag{44}$$

The perturbation method is then applied to equations (43) and (44). Let

$$\sigma(z) = \sigma^{(0)}(z) + \varepsilon\sigma^{(1)}(z) \tag{45}$$

$$\hat{V}(z) = \hat{V}^{(0)}(z) + \varepsilon\hat{V}^{(1)}(z) + \varepsilon^2\hat{V}^{(2)}(z) + \cdots \tag{46}$$

where ε is an arbitrary small real number. Substituting equations (45) and (46) into (43) and (44) and equating coefficients of powers of ε, we obtain the series of equations

$$\left.\begin{aligned}
&\frac{d^2\hat{V}^{(0)}}{dz^2} + \frac{1}{\sigma^{(0)}}\frac{d\sigma^{(0)}}{dz}\frac{d\hat{V}^{(0)}}{dz} - k^2\hat{V}^{(0)} = 0,\\
&\frac{d^2\hat{V}^{(1)}}{dz^2} + \frac{1}{\sigma^{(0)}}\frac{d\sigma^{(0)}}{dz}\frac{d\hat{V}^{(1)}}{dz} - k^2\hat{V}^{(1)} = k^2\frac{\sigma^{(1)}}{\sigma^{(0)}}\hat{V}^{(0)} - \frac{\sigma^{(1)}}{\sigma^{(0)}}\frac{d^2\hat{V}^{(0)}}{dz^2}\\
&\qquad\qquad - \frac{1}{\sigma^{(0)}}\frac{d\sigma^{(1)}}{dz}\frac{d\hat{V}^{(0)}}{dz},\\
&\frac{d^2\hat{V}^{(2)}}{dz^2} + \frac{1}{\sigma^{(0)}}\frac{d\sigma^{(0)}}{dz}\frac{d\hat{V}^{(2)}}{dz} - k^2\hat{V}^{(2)} = k^2\frac{\sigma^{(1)}}{\sigma^{(0)}}\hat{V}^{(1)} - \frac{\sigma^{(1)}}{\sigma^{(0)}}\frac{d^2\hat{V}^{(1)}}{dz^2}\\
&\qquad\qquad - \frac{1}{\sigma^{(0)}}\frac{d\sigma^{(1)}}{dz}\frac{d\hat{V}^{(1)}}{dz},\\
&\quad\vdots
\end{aligned}\right\} \tag{47}$$

The boundary conditions to be satisfied are

$$\left.\begin{aligned}
&\frac{d\hat{V}^{(0)}}{dz} = -\frac{I}{2\pi\sigma_s} \quad \text{at } z = 0 \text{ and } \hat{V}^{(0)} = 0 \text{ as } z \to \infty,\\
&\frac{d\hat{V}^{(1)}}{dz} = 0 \qquad \text{at } z = 0 \text{ and } \hat{V}^{(1)} = 0 \text{ as } z \to \infty,\\
&\frac{d\hat{V}^{(2)}}{dz} = 0 \qquad \text{at } z = 0 \text{ and } \hat{V}^{(2)} = 0 \text{ as } z \to \infty,\\
&\quad\vdots
\end{aligned}\right\} \tag{48}$$

If the equation for $\hat{V}^{(0)}$ with boundary conditions can be solved, then in many cases the following successive corrections in the perturbation series of $\hat{V}$ can be obtained recursively and $\hat{V}$ can be determined. In order to directly calculate the successive approximations, one has to know the Green function of the operator

$$\frac{d^2}{dz^2} + \frac{1}{\sigma^{(0)}} \frac{d\sigma^{(0)}}{dz} \frac{d}{dz} - k^2 \quad .$$

Since this function is not readily obtained for a given σ_0 an alternative perturbation approach using a simpler Green function will be used in the following.

(ii) Runge-Kutta Method

The solution of equation (43) or the $\hat{V}^{(0)}$ equation in the set of equations (47) will be derived by the Runge-Kutta method. For the three layer case described later these equations are simplified and can be solved analytically. A detailed treatment of the Runge-Kutta method is given in Collatz (1960). In the following only a short description of the method is presented and the formulas used directly in this thesis are tabulated.

Suppose the n^{th} order differential equation

$$y^{(n)} = f(x, y, y', \ldots, y^{(n-1)})$$

is to be integrated subject to initial values

$$y_o^{(\nu)} = y^{(\nu)}(x_o) \qquad \nu = 0, 1, 2, \ldots, n-1 \ ,$$

at the point $x = x_0$. Approximate values for y and its derivatives $y^{(\nu)}$ at $x_1 = x_0 + \Delta x$ can be obtained by using a Taylor series expansion truncated at the terms $y_0^{(n-1)}$,

$$y_0^{(\nu)} + \frac{\Delta x}{1!} y_0^{(\nu+1)} + \frac{(\Delta x)^2}{2!} y_0^{(\nu+2)} + \cdots + \frac{(\Delta x)^{n-\nu-1}}{(n-\nu-1)!} y_0^{(n-1)} = T_\nu(1) .$$

The value of the ν^{th} derivative $y^{(\nu)}$ at x_1 is obtained from

$$y_1^{(\nu)} = T_\nu(1) + \frac{\nu!}{(\Delta x)^\nu} k^{(\nu)} \qquad \nu = 0, 1, 2, \ldots, n-1$$

where the corrections $k^{(\nu)}$ are chosen to be linear combinations

$$k^{(\nu)} = \sum_{\rho=1}^{r} \gamma_{\nu\rho} k_\rho \qquad \nu = 0, 1, 2, \ldots, n-1$$

of certain auxiliary quantities $k_1, k_2, k_3, \ldots, k_r$. For the second order equations these quantities and calculation procedures are given in the following table.

Table 2. Runge-Kutta scheme for differential equations of the second order $y'' = f(x, y, y')$.

x	y	$(\Delta x)y' = v_1$	$k_\nu = \frac{(\Delta x)^2}{2} f(x, y, \frac{v_1}{\Delta x})$	Correction
x_0	y_0	v_{10}	k_1	$k = \frac{1}{3}(k_1 + k_2 + k_3)$
$x_0 + \frac{1}{2}(\Delta x)$	$y_0 + \frac{1}{2}v_{10} + \frac{1}{4}k_1$	$v_{10} + k_1$	k_2	
$x_0 + \frac{1}{2}(\Delta x)$	$y_0 + \frac{1}{2}v_{10} + \frac{1}{4}k_1$	$v_{10} + k_2$	k_3	$k' = \frac{1}{3}(k_1 + 2k_2 + 2k_3 + k_4)$
$x_0 + \Delta x$	$y_0 + v_{10} + k_3$	$v_{10} + 2k_3$	k_4	
$x_1 = x_0 + \Delta x$	$y_1 = y_0 + v_{10} + k$	$v_{11} = v_{10} + k'$		

The approximate values of y and its derivatives at the point $x_1 = x_0 + \Delta x$ are used as starting values for the next step of calculation, i.e., for the evaluation of y and its derivatives at $x_2 = x_0 + 2(\Delta x)$. As stated by Collatz (1960), a rough guide for finding a reasonable value of Δx is that it should be chosen such that $k_2 - k_3$ does not exceed $k_1 - k_2$ in magnitude more than a few percent. In practice the step length Δx can also be determined by trial and error. If Δx is shortened and the integration results don't change, the step length needs not be shortened any more. The error in the calculation with steps of length Δx should be roughly $\frac{1}{15}$ of the difference between the results of this calculation and those of the calculation with steps of length $2(\Delta x)$.

The problem at hand is to solve a second order differential equation numerically with two boundary conditions (refer to equations (43) and 44):

$$\frac{d^2\hat{V}}{dz^2} + \frac{1}{\sigma(z)} \frac{d\sigma(z)}{dz} \frac{d\hat{V}}{dz} - k^2\hat{V} = 0 \qquad (43)$$

$$\frac{d\hat{V}}{dz} = -\frac{I}{2\pi\sigma_s} \text{ at } z = 0 \text{ and } \hat{V} = 0 \text{ as } z \to \infty \ . \qquad (44)$$

The second boundary condition $\hat{V} = 0$ as $z \to \infty$ is replaced by a fixed boundary condition at $z = z'$ and below z' (i.e., $z > z'$) a uniform conductivity of the ground is assumed. The numerical calculation can thus be carried out. At $z = 0$, the upper boundary, $\hat{V}'$ is fixed and $\hat{V}$ is varied until the numerical integration step by step results in the prescribed values at $z = z'$. The calculation procedure has been

programmed by the author so that the Runge-Kutta method stated above can be carried out on the computer. A case has been solved using this method for a Gaussian conductivity profile and will be shown later in this chapter.

(iii) Solution to the Perturbation Equation

Assuming that $\hat{V}^{(0)}$ has been obtained by the above method the solutions of the second, third, ... etc. equations of the set (47) require the knowledge of the Green function of the operator

$$\frac{d^2}{dz^2} + \frac{1}{\sigma^{(0)}} \frac{d\sigma^{(0)}}{dz} \frac{d}{dz} - k^2 . \tag{49}$$

Since this function is difficult to derive an alternative technique will be applied in the following. This involves the solving of an integral equation, the Fredholm equation of the second kind. Define $L = -k^2 + (d^2/dz^2)$ then the second equation of (47) can be written

$$L\hat{V}^{(1)} = - \frac{D\sigma^{(0)}}{\sigma^{(0)}} D\hat{V}^{(1)} - \frac{\sigma^{(1)}}{\sigma^{(0)}} L\hat{V}^{(0)} - \frac{D\sigma^{(1)}}{\sigma^{(0)}} D\hat{V}^{(0)} . \tag{50}$$

The same applies to the higher order equations. The boundary conditions associated with equation (50) are (refer to the second equation of (48))

$$D\hat{V}^{(1)} = 0 \text{ at } z = 0 \text{ and } \hat{V}^{(1)} = 0 \text{ as } z \to \infty . \tag{51}$$

The Green function of L can easily be found (similar to that of a step shelf model case in the problem of the dynamics of deep sea currents

discussed on page 29) by solving the equation

$$LG = \delta(z - z')$$

with boundary conditions DG = 0 at z = 0 and G = 0 as $z \to \infty$ and the continuity of G and DG at z = z' (see the diagram below).

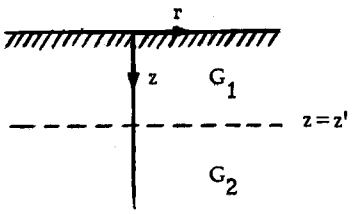

The Green function thus obtained is

$$\left.\begin{aligned} G_1(z, z') &= -\frac{1}{2k}[\exp(kz) + \exp(-kz)]\exp(-kz') \text{ for } z < z' \\ G_2(z, z') &= -\frac{1}{2k}[\exp(kz') + \exp(-kz')]\exp(-kz) \text{ for } z > z' \ . \end{aligned}\right\} \quad (52)$$

The solution of equation (50) can then formally be written as

$$\hat{V}^{(1)} = \int_0^\infty G_2(z, z')\left[a\frac{d\hat{V}^{(1)}(z')}{dz'} + bL\hat{V}^{(0)}(z') + c\frac{d\hat{V}^{(0)}(z')}{dz'}\right] dz' \quad (53)$$

where $a = -(D\sigma^{(0)})/\sigma^{(0)}$, $b = -\sigma^{(1)}/\sigma^{(0)}$, and $c = -(D\sigma^{(1)})/\sigma^{(0)}$. By setting

$$A(z) = \int_0^\infty G_2(z, z')\left[b\ L\ \hat{V}^{(0)}(z') + c\frac{d\hat{V}^{(0)}(z')}{dz'}\right] dz' \ ,$$

equation (53) results in

$$\hat{V}^{(1)} = A(z) + \int_0^\infty G(z, z')\ a(z')\frac{d\hat{V}^{(1)}(z')}{dz'}\ dz' \ .$$

Applying integration by parts one reaches the final form for $\hat{V}^{(1)}$

$$\hat{V}^{(1)}(z) = B(z) - \int_0^\infty H(z, z')\ \hat{V}^{(1)}(z')\ dz' \quad (54)$$

where $B(z) = A(z) - G(z, 0)\ a(0)\hat{V}^{(1)}(0)$ and $H(z, z') = d\{G(z, z')a(z')\}/dz'$.

This is a Fredholm equation of the second kind and various methods

can be employed to solve it (Mikhlin and Smolitskiy, 1967). One of the most common ones is the iteration method where the free term $A(z)$ is used as the first approximation to $\hat{V}^{(1)}(z)$.

It is worthwhile to note here that the Green function of the operator (49) can be obtained by approximating the conductivity profile $\sigma^{(0)}(z)$ by a number of small segments with constant conductivity. The Green function can thus be obtained through recursive relations.

(iv) Hankel Transform

After the calculations of $\hat{V}^{(1)}(z)$ and the following successive corrections $\hat{V}^{(2)}(z)$, $\hat{V}^{(3)}(z)$, . . . , in the perturbation series for $\hat{V}(z)$ the inverse Hankel transform has to be carried out

$$V(r, z) = \int_0^\infty \hat{V}(k, z) J_o(kr) k \, dk$$

so that $V(r, z)$ and the apparent resistivity can be obtained. In using the Wenner configuration the apparent resistivity ρ_a is

$$\rho_a = \frac{2\pi d}{I} \Delta V \tag{55}$$

where d is the distance between the electrodes and ΔV the electrical potential difference between the two central electrodes. The numerical computations of Hankel transform and inverse Hankel transform are here carried out on the basis of a method proposed by Longman (1956, 1957). The method is briefly described as follows. Assume that the integral

$$\int_0^\infty J_o(x)\, g(x)\, dx \tag{56}$$

is to be computed numerically, where g(x) is a well-behaved continuous function which tends to a finite constant value or zero as x tends to infinity. Moreover, assume that the integral over each half-cycle is smaller in absolute magnitude than (and opposite in sign to) that over the preceding half-cycle. The method also applies in the case where after a finite number of half-cycles the above assumption holds. Two main steps are involved in the calculation. The first step involves performing the integration over each of the first twenty half-cycles, i.e., evaluating the integrals

$$\int_{x_i-1}^{x_i} J_o(x)\, g(x)\, dx \qquad i = 1,\ 2,\ \ldots,\ 20 \tag{57}$$

where x_0 is zero and x_i is the i^{th} zero of $J_o(x)$. The first twenty terms of a slowly convergent alternating series for the integral (56) are obtained. The second step involves applying the Euler transformation to the alternating series just obtained in order to obtain a rapidly convergent series for the numerical value of (56). In order to get high accuracy for the calculation, the Gaussian quadrature formula is used for the integrals (57) for sixteen points of subdivision of each interval $[x_i,\ x_i+1]$. According to Gauss' method of numerical integration, an integral is approximated by a series

$$\int_{-1}^{-1} f(x)\, dx \sim a_1 f(x_1) + a_2 f(x_2) + \cdots + a_n f(x_n)\ . \tag{58}$$

This formula is exact when f(x) is a polynomial of a degree 2n-1.

The x_n's and the coefficients a_n's are then determined by

$$\int_{-1}^{1} x^k dx = a_1 x_1^k + a_2 x_2^k + \cdots + a_n x_n^k, \quad k = 0, 1, \ldots, 2n-1 . \tag{59}$$

The x_n's are now chosen to be the n zeros of $P_n(x)$, the Legendre polynomial of degree n (Milne, 1949). The coefficients a_n's then can be determined by the first n equations of equations (59). For a given value of n, Gauss' formula provides an approximation equivalent to replacing the integrand by a polynomial of degree 2n-1. The abscissae, the zeros of the Legendre polynomial, and the associated coefficients are tabulated in "NBS Applied Mathematics Series, No. 37, 1954", Davis and Rabinowitz (1956), and Abramovitz and Stegun (1961). The coefficients for sixteen subdivision points of each interval are tabulated as follows:

Table 3. Gauss integration coefficients.

.02715 24594
.06225 35239
.09515 85117
.12462 89713
.14959 59888
.16915 65194
.18260 34150
.18945 06105
.18945 06105
.18260 34150
.16915 65194
.14959 59888
.12462 89713
.09515 85117
.06225 35239
.02715 24594

For any interval of integration [p, q] the formula (58) is converted to

$$\int_p^q f(x)\,dx = \frac{q-p}{2} \sum_{i=1}^{n} a_i\, f\left(x_i \frac{q-p}{2} + \frac{q+p}{2}\right).$$

For the integrations of the first twenty half-cycles,

$$\int_{x_{i-1}}^{x_i} J_o(x)\, g(x)\,dx \qquad i = 1,\ 2,\ \ldots,\ 20 \tag{57}$$

all the abscissae and the associated $J_o(x)$ values are tabulated by Longman (1957), which in turn are calculated by the formula

$$x_i = x_i^1 \frac{q-p}{2} + \frac{q+p}{2}$$

where x_i are abscissae in the interval [p, q], and x_i^1 are those in the interval [-1, 1] (NBS Applied Mathematics Series, No. 37, 1954). Interpolations are carried out by means of the first four terms of the Taylor's series expansion from Harvard University tables (1947). The results of Longman (1957) are also plotted in Figure 8.

Thus the integration (56) is approximated by a slowly convergent alternating series of twenty terms. The Euler transformation is then applied to this series in order to obtain a rapidly convergent series and give a better approximation to the integral (56) (Bromwich, 1926). According to this transformation, if one has a series

$$H_0 - H_1 + H_2 - H_3 + H_4 - \ldots \tag{60}$$

where $H_n > 0$, $H_{n+1} < H_n$ for all n, and writes

$$\Delta H_n = H_{n+1} - H_n, \quad \Delta^{r+1} H_n = \Delta^r H_{n+1} - \Delta^r H_n$$

then

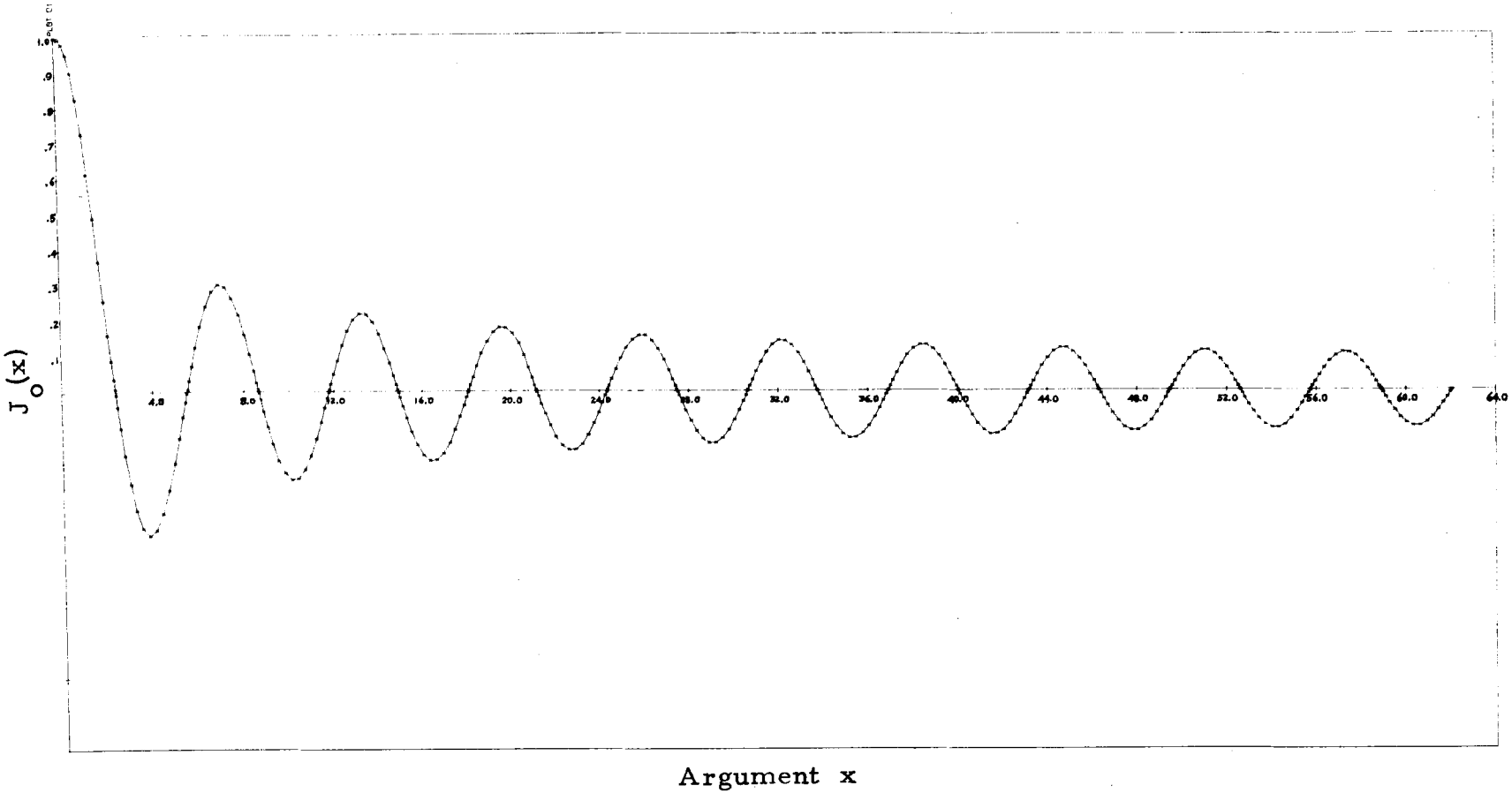

Figure 8. Abscissae and the corresponding values of $J_0(x)$, the Bessel function of the first kind of order zero, for the Gaussian integration formula for the first twenty half-cycles of $J_0(x)$.

$$\sum_{0}^{\infty} (-1)^n H_n = \frac{1}{2} H_0 - \frac{1}{4} \Delta H_0 + \frac{1}{8} \Delta^2 H_0 - \cdots \quad . \tag{61}$$

In equation (61) the series on the right hand side can be shown to be convergent whenever the original series (60) is (Ames, 1902); i.e., if the series (60) converges, it can be shown that the remainder of the series at the right hand side of (61) after n terms, R_n, approaches to zero as n approaches infinity. R_n can be estimated by the formula (Bromwich, 1926)

$$\left|R_n\right| < 2^{-n} \left|\Delta^n H_0\right| \quad .$$

Following the steps described above, the result can be concluded as follows. Let x_i be the zeros of $J_o(x)$, the integral (56) can be split up as

$$\int_0^{\infty} J_o(x)g(x)\,dx = \int_0^{x_1} J_o(x)g(x)\,dx - \int_{x_1}^{x_2} J_o(x)g(x)\,dx + \int_{x_2}^{x_3} J_o(x)g(x)\,dx - \cdots$$

$$= \int_0^{x_1} J_o(x)g(x)\,dx - (H_o - H_1 + H_2 - H_3 + H_4 - \cdots)$$

where

$$H_o - H_1 + H_2 - H_3 + H_4 - \cdots$$

is a slowly convergent alternating series. Then according to the Euler transformation

$$\int_0^{\infty} J_o(x)g(x)\,dx = \int_0^{x_1} J_o(x)g(x)\,dx - (\tfrac{1}{2}H_o - \tfrac{1}{4}\Delta H_o + \tfrac{1}{8}\Delta^2 H_o - \cdots\cdots) .$$

This method has also been programmed by the author using FORTRAN IV language so that the Hankel transform can be carried out fast on the CDC 3300 computer at Oregon State University.

(v) Examples

To demonstrate the above computational technique the well known cases of the uniform and the two-layer conductivity models (Van Nostrand and Cook, 1966) will be treated using the Runge-Kutta method and the Hankel transformations. Also a more complicated case in which $\sigma(z)$ is a Guassian distribution curve is also investigated. The results turn out to be satisfactory when compared to the exact analytic solutions which are available in the uniform and the two-layer cases.

(a) The one layer case (refer to the diagram below).

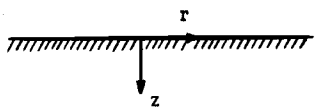

σ = constant

The solution to the equation (43) with boundary conditions is simply

$$\hat{V}(z) = \frac{I}{2\pi\sigma k} \exp(-kz) \quad . \tag{62}$$

The equation to be integrated by the Runge-Kutta method is

$$\frac{d^2\hat{V}}{dz^2} - k^2\hat{V} = 0 \quad .$$

The boundary condition at z = 0 is

$$\frac{d\hat{V}}{dz} = -\frac{I}{2\pi\sigma} \quad .$$

The value of $\hat{V}$ at z = 0 is varied such that after a series of step by step integrations using a step length of 10^{-4}, $\hat{V}(z)$ and $d\hat{V}(z)/dz$ become proportional to prescribed values at a fixed depth which has been normalized to 1. The Runge-Kutta method turns out to be successful, the values at and below the surface are identical to those of the exact solutions (62). In this case the inverse Hankel transform of (62) is trivial (Duff and Naylor, 1966),

$$V(r, z) = \frac{I}{2\pi\sigma\sqrt{r^2 + z^2}} \quad ,$$

so that the numerical Hankel transform technique is not used here.

(b) The two layer case (refer to the diagram below).

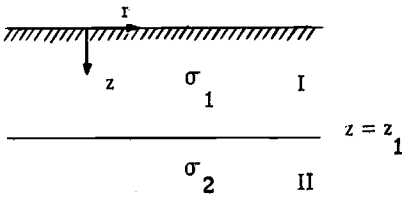

The equation to be solved in this case is also

$$\frac{d^2\hat{V}}{dz^2} - k^2\hat{V} = 0 \quad . \qquad (63)$$

The boundary conditions are

$$\frac{d\hat{V}}{dz} = -\frac{I}{2\pi\sigma_1} \quad \text{at } z = 0, \quad \hat{V} = 0 \text{ as } z \to \infty ,$$

and

$$\hat{V} \text{ and } \sigma\frac{d\hat{V}}{dz} \text{ are continuous at } z = z_1 .$$

After some algebra the analytical exact solutions are

$$\left.\begin{aligned} \hat{V}_I &= \frac{I}{2\pi\sigma_1 k}\left[\left(1 + \frac{\mu_{12}}{\exp(2kz_1)-\mu_{12}}\right)\exp(-kz) + \frac{\mu_{12}}{\exp(2kz_1)-\mu_{12}}\exp(kz)\right] \\ \hat{V}_{II} &= \frac{I}{2\pi\sigma_1 k}\left[1 + (1 + \exp(2kz_1))\frac{\mu_{12}}{\exp(2kz_1) - \mu_{12}}\right]\exp(-kz) \end{aligned}\right\} \tag{64}$$

where $\mu_{12} = (\sigma_1 - \sigma_2)/(\sigma_1 + \sigma_2)$. This set of solutions is given by Grant and West (1965), although their derivation is slightly different.

The Runge-Kutta method is used to integrate equation (63). The boundary condition is

$$\frac{d\hat{V}}{dz} = -\frac{I}{2\pi\sigma_1} \quad \text{at } z = 0$$

and $\hat{V}$ at $z = 0$ is varied again such that after integrations step by step the values of $\hat{V}$ and $d\hat{V}/dz$ at $z = z_1$ are identical to the prescribed boundary conditions,

$$\hat{V} = \text{constant x } \exp(-kz_1) , \quad \frac{d\hat{V}}{dz} = \text{constant x } (-k) \text{ x } \exp(-kz_1) .$$

The numerical integration results of $\hat{V}$ and $d\hat{V}$ are compared with those from the exact solution (64) and they are identical. When z_1 is normalized to one and $k = 1$, after a few trials it is found that the best

integration step length is 10^{-2}. However, when k is increased, the optimum step length becomes smaller, viz, 10^{-3} or 10^{-4}. The numerical Hankel transform technique mentioned in (iv) is then applied to $\hat{V}$. The results with regard to V and the apparent resistivities (refer to equation (55)) turn out to be the same as those obtained by Roman (1941) using the image method and by Mooney and Wetzel (1956). Their results of apparent resistivity curves are reproduced (Figure 9).

(c) The Gaussian conductivity profile case (refer to the diagram below and Figure 10).

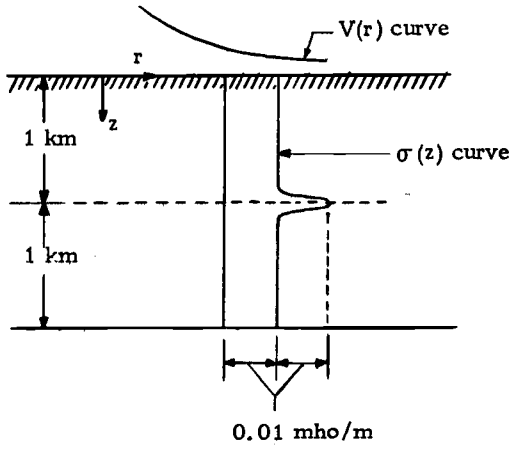

The electric conductivity curve is assumed to be a Gaussian type function,

$$\sigma(z) = 10 \exp[-100\,\pi(z-1)^2] + 10 \quad \text{mho/km} .$$

It is noted that for this curve

$$\int_{-\infty}^{\infty} [\sigma(z) - 10]\, dz = 1 \text{ mho and } \overline{(\Delta z)^2} = \frac{100}{\sqrt{2\pi}}\ \Omega\,\text{m} .$$

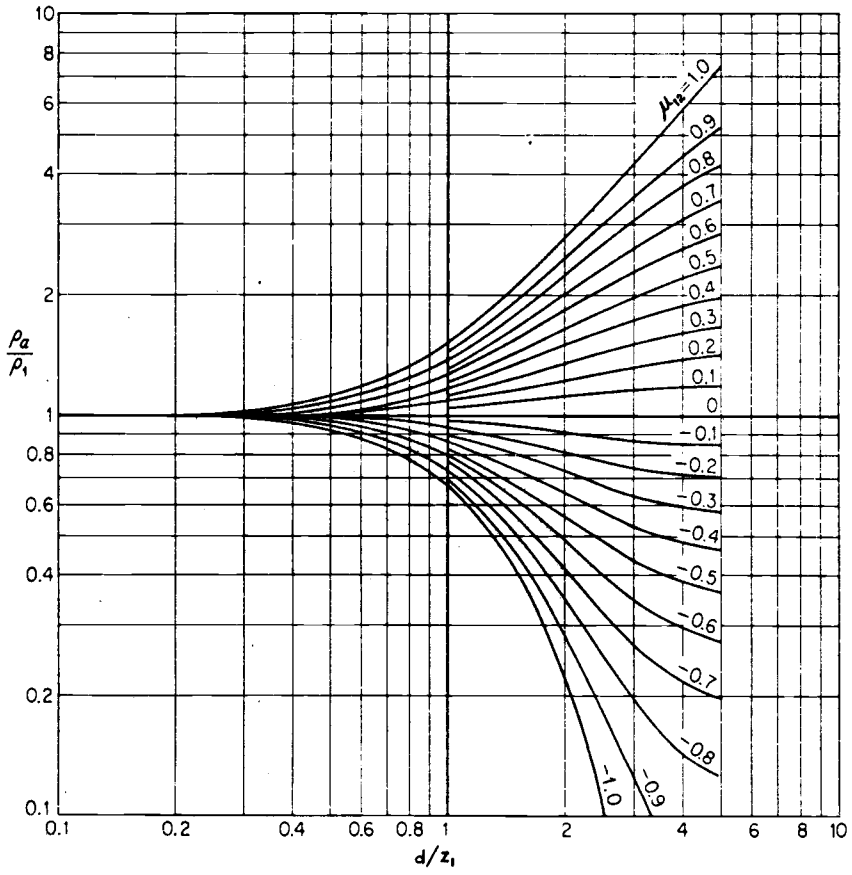

Figure 9. Apparent resistivity curves for the two-layer model using the Wenner configuration (After Mooney and Wetzel (1956)), where d is the distance between electrodes. $\rho_1 = 1/\sigma_1$.

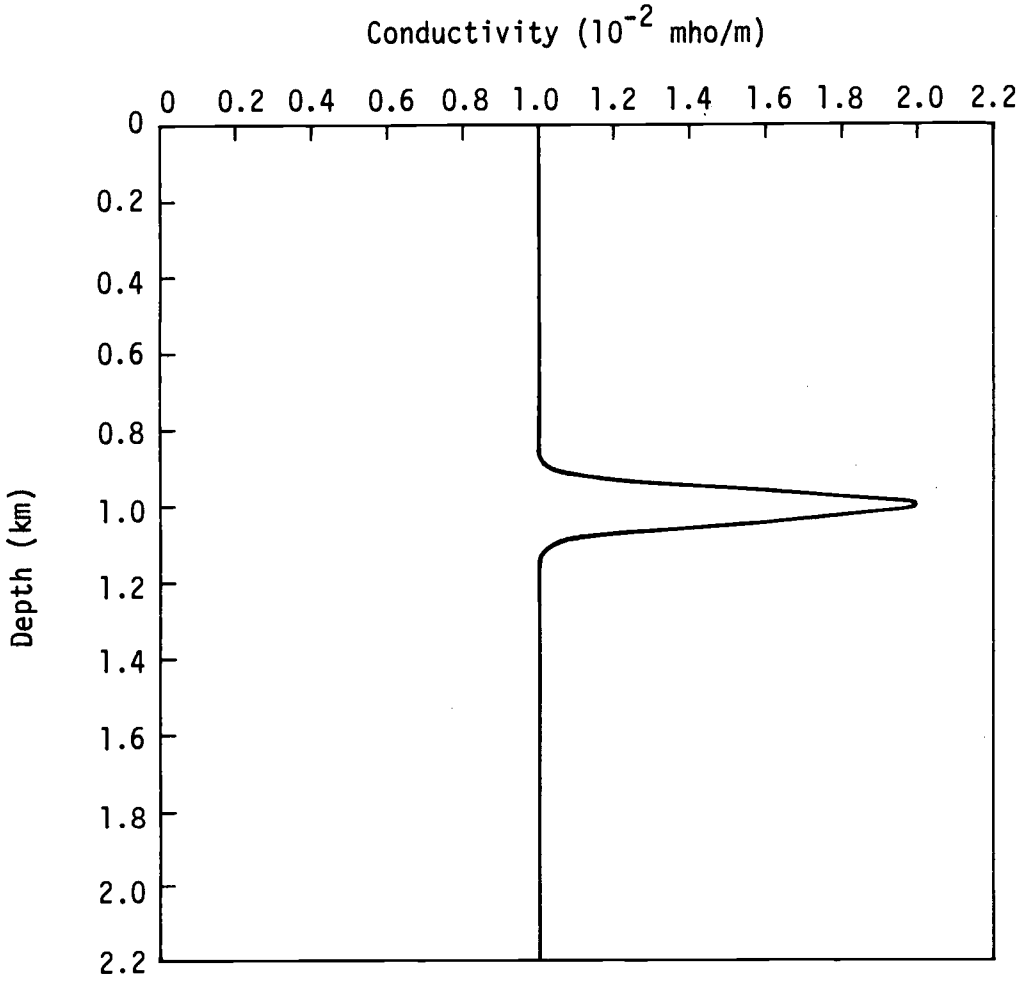

Figure 10. The Gaussian conductivity profile.

The equation to be solved is

$$\frac{d^2\hat{V}}{dz^2} + \frac{1}{\sigma(z)} \frac{d\sigma(z)}{dz} \frac{d\hat{V}}{dz} - k^2\hat{V} = 0 , \qquad (65)$$

and the boundary conditions associated with it are

$$\frac{d\hat{V}}{dz} = - \frac{I}{2\pi\sigma_s} \text{ at } z = 0 \text{ and } \hat{V} = 0 \text{ as } z \to \infty ,$$

where σ_s is the conductivity at $z = 0$, the surface. This equation (65) with the boundary conditions cannot be solved analytically. Since $\sigma(z)$ tends to 0.01 mho/m very fast as z becomes large, it is assumed that $\sigma(z) = 0.01$mho/m for $z \geq 2$ km. Because of this assumption, the boundary conditions at $z = 2$ km are

$$\hat{V}(z) = \text{constant} \times \exp(-kz) \text{ and } \frac{d\hat{V}}{dz} = \text{constant} \times (-k) \times \exp(-kz)$$

(refer to (a) and (b) above). The Runge-Kutta method is then used to solve the equation (65). Again the condition

$$\frac{d\hat{V}}{dz} = - \frac{I}{2\pi\sigma_s} \text{ at } z = 0$$

provides one of the boundary values for the integration. Proceeding with a variable $\hat{V}$ at $z = 0$ the integration is stopped when the values

$$\hat{V} \text{ and } \frac{d\hat{V}}{dz} \text{ at } z = 2 \text{ km}$$

are proportional to the prescribed boundary conditions at $z = 2$ km. After some trials it is found, as in the one and two layer cases, that the best step length of integration for $k = 1.088$ or less is 10^{-2} km.

For larger k values the required step length has to be reduced in order to get reasonable results. When $k = 7.236$ the best integration step length is 10^{-3} km. Upon the application of the inverse Hankel transform to the results from the Runge-Kutta method it is found that the electric potential V at r = 1 km and 2 km is 2.8% lower than in the uniform conductivity case (i.e., $\sigma = 0.01$ mho/m uniformly). These results are consistent with those calculated by an approximate three-layer model, which will be described in detail below.

(vi) Direct Method for the General Case

The purpose of the direct method is to derive the conductivity distribution on the basis of the surface measurements of the electric potentials V or the apparent resistivities. In the case of the perturbation method applied in the present work this implies that the term $\varepsilon\sigma^{(1)}(z)$ in equation (45) has to be determined by the surface observations. Only the second order equation, the second equation of equations (47), is considered in detail here. Derivations of the direct methods for higher order equations are similar to the derivation for the second order equation. Equation (54) rewritten is

$$\hat{V}^{(1)}(z) = B(z) - \int_0^\infty H(z, z')\, \hat{V}^{(1)}(z')dz' \qquad (54)$$

where $B(z) = A(z) - G(z, 0)a(0)\, \hat{V}^{(1)}(0)$, $H(z, z') = \frac{d}{dz'}\{ G(z, z')a(z') \}$, and A(z), G(z, z') and a(z) are the same as defined before, i.e.,

$$A(z) = \int_0^\infty G(z, z') \left[b\, L\hat{V}^{(0)}(z') + c \frac{d\hat{V}^{(0)}(z')}{dz'} \right] dz'$$

$$a(z) = - \frac{D\sigma^{(0)}}{\sigma^{(0)}} , \quad b = - \frac{\sigma^{(1)}}{\sigma^{(0)}} , \quad c = - \frac{D\sigma^{(1)}}{\sigma^{(0)}}$$

$$G(z, z') = \begin{cases} G_1 = - \frac{1}{2k} [\exp(kz) + \exp(-k z)] \exp(-k z') & \text{for } z < z' \\ G_2 = - \frac{1}{2k} [\exp(kz') + \exp(-kz')] \exp(-kz) & \text{for } z > z' \end{cases}$$

Assuming $z = 0$ in (54) we have

$$\hat{V}^{(1)}(0) = B(0) - \int_0^\infty H(0, z')\, \hat{V}^{(1)}(z')\, dz' \,. \tag{66}$$

where $B(0)$ is,

$$B(0) = A(0) - G(0, 0) a(0)\, \hat{V}^{(1)}(0)$$

$$= - \frac{1}{k} \int_0^\infty \exp(-k z') \left\{ - \frac{\sigma^{(1)}}{\sigma^{(0)}} \left(- k^2 \hat{V}^{(0)} + \frac{d^2 \hat{V}^{(0)}}{dz'^2} \right) - \frac{1}{\sigma^{(0)}} \frac{d\sigma^{(1)}}{dz'} \frac{d\hat{V}^{(0)}}{dz'} \right\} dz'$$

$$- \frac{1}{k} \left(\frac{1}{\sigma^{(0)}} \frac{d\sigma^{(0)}}{dz'} \right)_{\text{at } z' = 0} \hat{V}^{(1)}(0) \,. \tag{67}$$

The processing of the second term on the right hand side of (66) is as follows. At first, we will state a theorem for the asymptotic expansion of the Laplace integral (Erdélyi, 1956)

$$\psi(x) = \int_0^\infty \exp(-xt)\, \phi(t)\, dt \tag{68}$$

where x in general is a complex variable.

Definition. A function ϕ will be said to belong to $L(x_o)$ if the integral (68) exists, in the sense that

$$\lim_{T\to\infty} \int_0^T \exp(-xt)\, \phi(t)\, dt$$

is finite for $x = x_o$.

Definition. S_Δ is the sector $0 < |x| < \infty$, $|\arg x| < \frac{\pi}{2} - \Delta$.

Theorem. If $\phi(t)$ is N times continuously differentiable for $0 \leq t < t_o$ and belongs to $L(x_o)$ for some x_o then

$$\psi(x) \sim \sum \phi^{(n)}(0)\, x^{-n-1}$$

to N terms, uniformly in arg x, as $x \to \infty$ in S_Δ, $\Delta > 0$.

The proof of the theorem, which is based on integrations by parts, is omitted here.

The direct method developed in this section is based on the requirement that this theorem holds. For the simplified case of a three-layer model discussed in the next section, this theorem is not a necessary condition for the direct method to work. The evaluation of the integral

$$\int_0^\infty H(0, z')\, \hat{V}^{(1)}(z')\, dz'$$

is then as follows. Since

$$H(0, z') = a(z') \frac{dG(0, z')}{dz'} + G(0, z') \frac{da(z')}{dz'}$$

and

$$G(0, z') = -\frac{1}{k} \exp(-k z'),$$

using the theorem stated above one has

$$\int_0^\infty H(0, z')V^{(1)}(z')dz' = [\frac{a(0)}{k} - \frac{(\frac{da(z')}{dz'})_{z'=0}}{k^2}]\hat{V}^{(1)}(0) + \text{Higher order term.} \tag{69}$$

Substituting (67) and (69) into (66) and defining that

$$\pi(z') = -\frac{\sigma^{(1)}}{\sigma^{(0)}}(-k^2\hat{V}^{(0)} + \frac{d^2\hat{V}^{(0)}}{dz'^2}) - \frac{1}{\sigma^{(0)}}\frac{d\sigma^{(1)}}{dz'}\frac{d\hat{V}^{(0)}}{dz'} \tag{70}$$

one has then

$$\int_0^\infty \exp(-kz')\pi(z')dz' = -k\hat{V}^{(1)}(0) - \frac{(a\frac{d\hat{V}^{(1)}}{dz'})_{z'=0}}{k} - \frac{[\frac{d}{dz'}(a\frac{d\hat{V}^{(1)}}{dz'})]_{z'=0}}{k^2}$$

$$- \frac{[\frac{d^2}{dz'^2}(a\frac{d\hat{V}^{(1)}}{dz'})]_{z'=0}}{k^3} - \cdots - \frac{[\frac{d^{n-1}}{dz'^{(n-1)}}(a\frac{d\hat{V}^{(1)}}{dz'})]_{z'=0}}{k^n} - \cdots . \tag{71}$$

The boundary condition at $z = 0$ is $d\hat{V}^{(1)}/dz = 0$ so that equation (71) is ultimately transformed into the following form:

$$\int_0^\infty \exp(-kz')\pi(z')dz' = -k\hat{V}^{(1)}(0) - \frac{[\frac{d}{dz'}(a\frac{d\hat{V}^{(1)}}{dz'})]_{z'=0}}{k^2} - \frac{[\frac{d^2}{dz'^2}(a\frac{d\hat{V}^{(1)}}{dz})]_{z'=0}}{k^3}$$

$$- \cdots - \frac{[\frac{d^{(n-1)}}{dz'^{(n-1)}}(a\frac{d\hat{V}^{(1)}}{dz'})]_{z'=0}}{k^n} - \cdots . \tag{72}$$

The left hand side of equation (72) appears as the Laplace transform of $\pi(z')$. The direct method solution for $\pi(z')$ can be obtained in the following way. In the zeroth order approximation we set the derivatives of $\hat{V}^{(1)}$ to zero at the right hand side of equation (72). This is equivalent to the approximation

$$\frac{d^n \hat{V}}{dz^n} \approx \frac{d^n \hat{V}^{(0)}}{dz^n} \quad , \quad n = 1, \ 2, \ 3, \ \ldots \quad .$$

Then the first order approximation of $\pi(z')$ can be found by the inverse Laplace transformation of the right hand side of (72). The higher order approximations of $\pi(z')$ can thus be attained by the iteration method. Then by an integration of (70) we can obtain $\sigma^{(1)}(z)$.

The method for the numerical inversion of the Laplace transform used in this thesis is that proposed by Piessens (1969). This method is an extension of Bellman's method (Bellman et al., 1966) and is equivalent to the method of Lanczos (Lanczos, 1956). For other methods of numerical inversion of the Laplace transform one is referred to Bellman et al. (1966) and Dubner and Abate (1968). The method by Piessens is briefly described below and followed by an example.

The Laplace transform

$$\int_0^\infty \exp(-st)\, f(t)\, dt = F(s) \tag{73}$$

is to be inverted. Substituting

$$\exp(-t) = u$$

(73) becomes

$$\int_0^1 u^{s-1}\, f(-\ln u)\, d\, u = F(s) \quad . \tag{74}$$

Using the Gauss' method of numerical integration (refer to p. 54) (74) yields

$$\sum_{i=1}^{N} a_i u_i^{s-1} f(-\ln u_i) \approx F(s)$$

where u_i is the i^{th} zero of the Legendre polynomial of degree N and a_i is the corresponding weight. Let s assume N different values, then this system of N linear equations can bo solved

$$f(t_i) \approx \sum_{k=1}^{N} a_{ik}^{(N)} F(k) \tag{75}$$

where

$$t_i = -\ln u_i \quad .$$

The inversion formula (75) gives only values of f(t) at nonequidistant points. A change of t scale by using the Lagrange interpolation formula will give values of f(t) at equidistant points

$$f(t) \approx \sum_{k=1}^{N} \varphi_k^{(N)}[\exp(-t)]\, F(k)$$

where $\varphi_k^{(N)}[x]$ is a polynomial of degree N-1. The formula for $\varphi_k^{(N)}[x]$ has been derived by Piessens (1969) and some numerical values have also been tabulated. The values of $\varphi_k^{(6)}[\exp(-t)]$ for t = 0. to t = 7. at an interval of 0.5 are used in the calculations in this thesis, both in the example given below and examples in the next section for a three-layer model case.

A simple example is given here showing the use of this technique to carry out the numerical inversion of the Laplace transform. Let

$\sigma^{(0)}$ be constant and

$$\sigma^{(1)}(z) = C \exp(-z) ,$$

where C is a constant. Using equation (72) $\hat{V}^{(1)}(0)$ can be derived as

$$\hat{V}^{(1)}(0) = -\frac{1}{k} \frac{I}{2\pi(\sigma^{(0)})^2} \int_0^\infty \exp(-2kz') \frac{d\sigma^{(1)}}{dz'} dz' \quad . \tag{76}$$

After the evaluation of the integral we have

$$\hat{V}^{(1)}(0) = \frac{IC}{2\pi(\sigma^{(0)})^2 k} \quad \frac{1}{1 + 2k} \quad . \tag{77}$$

Inversely, if we assume that (77) is the known data, then $d\sigma^{(1)}/dz'$ can be found by the inverse Laplace transform

$$\frac{d\sigma^{(1)}}{dz'} = -\frac{\pi(\sigma^{(0)})^2}{I} \quad \frac{1}{2\pi i} \int_{c_o - i\infty}^{c_o + i\infty} \exp(\eta z') \; \eta \hat{V}^{(1)}(0) \, d\eta$$

where c_o is a constant and $\eta = 2k$. The results obtained analytically and numerically using the technique described above are consistent and can be seen in the following listing. The analytic result is simply

$$\frac{d\sigma^{(1)}}{dz'} = -C \exp(-z') \quad .$$

z	$\frac{d\sigma^{(1)}}{dz} \times C^{-1}$ (numerical result)	$\frac{d\sigma^{(1)}}{dz} \times C^{-1}$ (analytic result)
0	$1.000000000 \times 10^{0}$	$1.000000000 \times 10^{0}$
.50	$6.065306514 \times 10^{-1}$	$6.065306597 \times 10^{-1}$
1.00	$3.678794428 \times 10^{-1}$	$3.678794411 \times 10^{-1}$
1.50	$2.231301576 \times 10^{-1}$	$2.231301601 \times 10^{-1}$
2.00	$1.353352963 \times 10^{-1}$	$1.353352832 \times 10^{-1}$
2.50	$8.208498358 \times 10^{-2}$	$8.208499861 \times 10^{-2}$
3.00	$4.978707246 \times 10^{-2}$	$4.978706836 \times 10^{-2}$
3.50	$3.019739687 \times 10^{-2}$	$3.019738342 \times 10^{-2}$
4.00	$1.831563562 \times 10^{-2}$	$1.831563888 \times 10^{-2}$
4.50	$1.110903173 \times 10^{-2}$	$1.110899653 \times 10^{-2}$
5.00	$6.737992167 \times 10^{-3}$	$6.737946999 \times 10^{-3}$
5.50	$4.086762666 \times 10^{-3}$	$4.086771438 \times 10^{-3}$
6.00	$2.478778362 \times 10^{-3}$	$2.478752176 \times 10^{-3}$
6.50	$1.503437757 \times 10^{-3}$	$1.503439192 \times 10^{-3}$
7.00	$9.118467569 \times 10^{-4}$	$9.118819655 \times 10^{-4}$

Application of the Perturbation Method to the Three Layer Model

The parameters for the three-layer model under investigation are shown in the following diagram

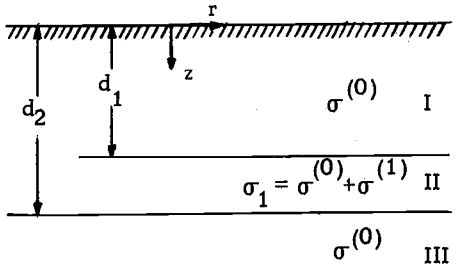

where $\sigma^{(0)}$ and $\sigma^{(1)}$ are constants. At first the exact solution of the problem is derived. The perturbation method is then used to obtain up to second order solutions. The results from the perturbation method are compared with those from the exact solution and conditions

for the validity of the perturbation method are discussed. Finally the direct method is treated.

(i) Exact Solution

Referring to the equation (41), since $\sigma^{(0)}$ and $\sigma^{(1)}$ are constants, the equation

$$\frac{\partial^2 V}{\partial r^2} + \frac{1}{r}\frac{\partial V}{\partial r} + \frac{\partial^2 V}{\partial z^2} = 0 \tag{78}$$

is to be solved with appropriate boundary conditions. Applying the Hankel transformation

$$\hat{V} = \int_0^\infty V(r, z)\, r\, J_o(kr)\, dr$$

equation (78) becomes

$$-k^2 \hat{V} + \frac{d^2 \hat{V}}{dz^2} = 0 \tag{79}$$

and the boundary conditions are

$$\left.\begin{aligned} &\frac{d\hat{V}}{dz} = -\frac{I}{2\pi\sigma^{(0)}} \quad \text{at } z = 0\,, \\ &\hat{V} = 0 \qquad \text{as } z \to \infty\,, \\ &\hat{V} \text{ and } \sigma\, \partial_z\, \hat{V} \text{ are continuous at } z = d_1 \text{ and } z = d_2\,. \end{aligned}\right\} \tag{80}$$

The solutions to equation (79) are

$$\hat{V}_I = A \exp(kz) + B \exp(-kz) \qquad \text{for region I}$$

$$\hat{V}_{II} = C \exp(kz) + D \exp(-kz) \qquad \text{for region II}$$

$$\hat{V}_{III} = E \exp(-kz) \qquad \text{for region III}\,.$$

When the boundary conditions (80) are incorporated and after some algebra the constants A, B, C, D, and E are determined and the solutions thus are

$$\hat{V}_I = \Lambda \exp(kz) + \frac{I}{2\pi\sigma^{(0)}k}$$

$$\times \frac{[\exp(-2kd_1)(\Sigma+1)^2 - \exp(-2kd_2)(\Sigma-1)^2]\exp(-kz)}{\exp(-2kd_1)(\Sigma+1)^2 - \exp(-2kd_2)(\Sigma-1)^2 - (\Sigma^2-1)\exp(-2kd_1)[\exp(-2kd_2)-\exp(-2kd_1)]}$$

$$\hat{V}_{II} = \frac{2\Lambda \exp(-2kd_2)}{(\Sigma+1)[\exp(-2kd_2)-\exp(-2kd_1)]} \exp(kz)$$

$$+ \frac{2\Lambda}{(\Sigma-1)[\exp(-2kd_2)-\exp(-2kd_1)]} \exp(-kz)$$

$$\hat{V}_{III} = \frac{4\Lambda\Sigma \exp(-kz)}{(\Sigma^2-1)[\exp(-2kd_2)-\exp(-2kd_1)]}$$

where

$$\Sigma = \frac{\sigma_1}{\sigma^{(0)}}$$

and

$$\Lambda = \frac{I}{2\pi\sigma^{(0)}k} \frac{(\Sigma^2-1)\exp(-2kd_1)[\exp(-2kd_2)-\exp(-2kd_1)]}{\exp(-2kd_1)(\Sigma+1)^2 - \exp(-2kd_2)(\Sigma-1)^2 - (\Sigma^2-1)\exp(-2kd_1)[\exp(-2kd_2)-\exp(-2kd_1)]}.$$

From $\hat{V}_I$ one has

$$\hat{V}(0) = \frac{I}{2\pi\sigma^{(0)}k} \frac{\exp(-2kd_1)(\Sigma+1)^2 - \exp(-2kd_2)(\Sigma-1)^2 + (\Sigma^2-1)\exp(-2kd_1)[\exp(-2kd_2)-\exp(-2kd_1)]}{\exp(-2kd_1)(\Sigma+1)^2 - \exp(-2kd_2)(\Sigma-1)^2 - (\Sigma^2-1)\exp(-2kd_1)[\exp(-2kd_2)-\exp(-2kd_1)]}$$

(81)

The inverse Hankel transform of equation (81) is performed by using the technique mentioned in the last section and V(0), the electric potentials on the surface and the apparent resistivities are obtained. The results are identical to those of Wetzel and McMurry (1937) and a sample of their apparent resistivity curves are reproduced (Figure 11).

(ii) Perturbation Solution

Since $\sigma^{(0)}$ is a constant the set of equations (47) is simplified to

$$\left.\begin{aligned}
&\frac{d\hat{V}^{(0)}}{dz^2} - k^2\hat{V}^{(0)} = 0 \\
&\frac{d^2\hat{V}^{(1)}}{dz^2} - k^2\hat{V}^{(1)} = -\frac{1}{\sigma^{(0)}}\frac{d\sigma^{(1)}}{dz}\frac{d\hat{V}^{(0)}}{dz} \\
&\frac{d^2\hat{V}^{(2)}}{dz^2} - k^2\hat{V}^{(2)} = \frac{\sigma^{(1)}}{(\sigma^{(0)})^2}\frac{d\sigma^{(1)}}{dz}\frac{d\hat{V}^{(0)}}{dz} - \frac{1}{\sigma^{(0)}}\frac{d\sigma^{(1)}}{dz}\frac{d\hat{V}^{(1)}}{dz} \\
&\quad\vdots
\end{aligned}\right\} \quad (82)$$

The boundary conditions to be satisfied remain the same as in equations (48),

$$\left.\begin{aligned}
&\frac{d\hat{V}^{(0)}}{dz} = -\frac{I}{2\pi\sigma^{(0)}} \text{ at } z = 0 \text{ and } \hat{V}^{(0)} = 0 \text{ as } z \to \infty, \\
&\frac{d\hat{V}^{(1)}}{dz} = 0 \qquad \text{at } z = 0 \text{ and } \hat{V}^{(1)} = 0 \text{ as } z \to \infty, \\
&\frac{d\hat{V}^{(2)}}{dz} = 0 \qquad \text{at } z = 0 \text{ and } \hat{V}^{(2)} = 0 \text{ as } z \to \infty, \\
&\quad\vdots
\end{aligned}\right\} \quad (83)$$

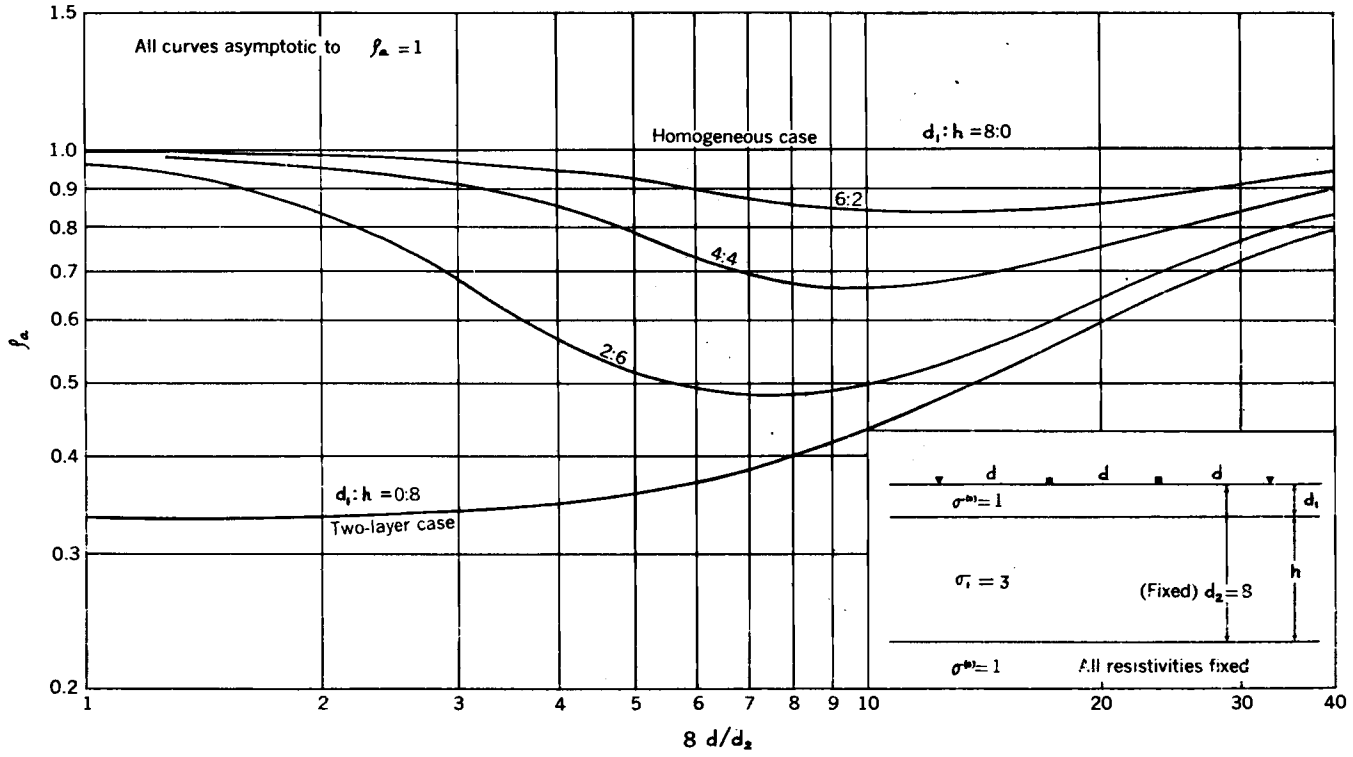

Figure 11. Apparent resistivity (ρ_a) curves of a three-layer model using the Wenner configuration (after Wetzel and McMurry (1937)).

Because interest centers on the apparent resistivities, the following derivations are devoted to the computation of V(0), the electric potentials on the surface, z = 0. The zeroth order solution, $V^{(0)}$ is simply the solution of a one-layer case of uniform conductivity $\sigma^{(0)}$ as derived before in the last section, which is

$$\hat{V}^{(0)}(z) = \frac{I}{2\pi\sigma^{(0)}k} \exp(-kz)$$

and

$$\hat{V}^{(0)}(0) = \frac{I}{2\pi\sigma^{(0)}k} \quad .$$

The first order correction, $V^{(1)}$ can be derived from knowledge of $\hat{V}^{(0)}(z)$, $\sigma^{(1)}$ and the Green function of the operator $(d^2/dz^2) - k^2$, which can be found in (iii) of the last section. The derivation of the correction is as follows (refer to equations (52) for G_1 and G_2).

For z in region I,

$$\hat{V}^{(1)}(z) = \int_0^z G_1 \left(-\frac{1}{\sigma^{(0)}} \frac{d\sigma^{(1)}}{dz'} \frac{d\hat{V}^{(0)}}{dz'}\right) dz' + \int_z^\infty G_2 \left(-\frac{1}{\sigma^{(0)}} \frac{d\sigma^{(1)}}{dz'} \frac{d\hat{V}^{(0)}}{dz'}\right) dz'$$

$$= -\frac{I}{4\pi\sigma^{(0)}k} \frac{\sigma^{(1)}}{\sigma^{(0)}} \{[\exp(-2kd_1) - \exp(-2kd_2)][\exp(kz) + \exp(-kz)]\}.$$

For z in region III

$$\hat{V}^{(1)}(z) = \int_0^z G_1 \left(-\frac{1}{\sigma^{(0)}} \frac{d\sigma^{(1)}}{dz'} \frac{d\hat{V}^{(0)}}{dz'}\right) dz' + \int_z^\infty G_2 \left(-\frac{1}{\sigma^{(0)}} \frac{d\sigma^{(1)}}{dz'} \frac{d\hat{V}^{(0)}}{dz'}\right) dz'$$

$$= -\frac{I}{4\pi\sigma^{(0)}k} \frac{\sigma^{(1)}}{\sigma^{(0)}} [\exp(-2kd_1) - \exp(-2kd_2)] \exp(-kz).$$

Hence $\hat{V}^{(1)}(0)$ at the surface of the ground is

$$\hat{V}^{(1)}(0) = -\frac{I}{2\pi\sigma^{(0)}k}\,\frac{\sigma^{(1)}}{\sigma^{(0)}}\left[\exp(-2kd_1) - \exp(-2kd_2)\right] . \qquad (84)$$

The second order correction $\hat{V}^{(2)}$ can again be derived from knowledge of $\hat{V}^{(0)}$, $\hat{V}^{(1)}$, $\sigma^{(1)}$ and the Green function of the operator $(d^2/dz^2) - k^2$.

The result is

$$\hat{V}^{(2)}(0) = \int_0^\infty G_1(0, z')\left(\frac{\sigma^{(1)}}{(\sigma^{(0)})^2}\,\frac{d\sigma^{(1)}}{dz'}\,\frac{d\hat{V}^{(0)}}{dz'} - \frac{1}{\sigma^{(0)}}\,\frac{d\sigma^{(1)}}{dz'}\,\frac{d\hat{V}^{(1)}}{dz'}\right) dz'$$

$$= \frac{I}{2\pi\sigma^{(0)}k}\left(\frac{\sigma^{(1)}}{\sigma^{(0)}}\right)^2\left[\exp(-2kd_1) - \exp(-2kd_2)\right]$$

$$+\frac{1}{k}\int_0^\infty \exp(-kz')\,\frac{1}{\sigma^{(0)}}\,\frac{d\sigma^{(1)}}{dz'}\,\frac{d\hat{V}^{(1)}}{dz'}\,dz'$$

$$= \frac{I}{2\pi\sigma^{(0)}k}\left(\frac{\sigma^{(1)}}{\sigma^{(0)}}\right)^2\left[\exp(-2kd_1) - \exp(-2kd_2)\right]$$

$$+\frac{1}{k}\,\frac{\sigma^{(1)}}{\sigma^{(0)}}\left\{\exp(-kd_1)\left(\frac{d\hat{V}^{(1)}}{dz'}\right)_{\text{at } z'=d_1}\right.$$

$$\left. - \exp(-kd_2)\left(\frac{d\hat{V}^{(1)}}{dz'}\right)_{\text{at } z'=d_2}\right\}$$

$$= \frac{I}{2\pi\sigma^{(0)}_k} \left(\frac{\sigma^{(1)}}{\sigma^{(0)}}\right)^2 [\exp(-2kd_1) - \exp(-2kd_2)]$$

$$+ \frac{I}{4\pi\sigma^{(0)}_k} \left(\frac{\sigma^{(1)}}{\sigma^{(0)}}\right)^2 [\exp(-2kd_1)-\exp(-2kd_2)][\exp(-2kd_1)-\exp(-2kd_2)-1]$$

$$= \frac{I}{4\pi\sigma^{(0)}_k} \left(\frac{\sigma^{(1)}}{\sigma^{(0)}}\right)^2 [\exp(-2kd_1)-\exp(-2kd_2)][\exp(-2kd_1)-\exp(-2kd_2)+1]. \quad (85)$$

The apparent resistivities calculated from perturbation solutions to the first and second order will now be compared with those calculated from the exact solutions. It is noted that the inverse Hankel transforms have to be applied to $\hat{V}^{(0)} + \hat{V}^{(1)}$ and $\hat{V}^{(0)} + \hat{V}^{(1)} + \hat{V}^{(2)}$ again before the apparent resistivities can be calculated. The numerical solutions are obtained for the following models. The parameters used, which have been nondimensionalized, are shown in the following diagram.

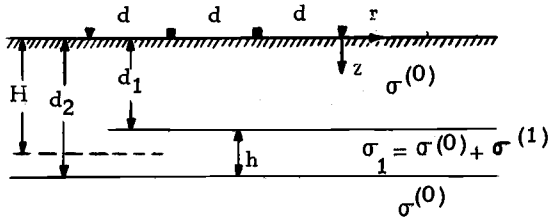

$H = \frac{1}{2}(d_1 + d_2)$

(a) Model A

$\sigma^{(0)} = 1, \quad d_2 = 1$

$$\sigma^{(1)} = \begin{bmatrix} 0.1 \\ 0.5 \\ 1. \\ 2. \end{bmatrix} \qquad d_1 = \begin{bmatrix} 0.9 \\ 0.7 \\ 0.5 \\ 0.3 \\ 0.1 \end{bmatrix} \qquad r = \begin{bmatrix} 0.25 \\ 0.5 \\ 1. \\ 2. \\ 4. \\ 8. \\ 16. \end{bmatrix}$$

(b) Model B

$\sigma^{(0)} = 2, \quad d_2 = 6$

$$\sigma^{(1)} = \begin{bmatrix} 0.4 \\ 2. \\ 4. \\ 10. \end{bmatrix} \qquad d_1 = \begin{bmatrix} 5. \\ 4. \\ 3. \\ 2. \\ 1. \end{bmatrix} \qquad r = \begin{bmatrix} 0.5 \\ 1. \\ 2. \\ 4. \\ 8. \\ 16. \\ 32. \end{bmatrix}$$

(c) Model C

$$\frac{\sigma^{(1)}_h}{\sigma^{(0)}_H} = 0.2,\ 0.05;\ d_2 = 1$$

$$h = \begin{bmatrix} 5.0 \times 10^{-3} \\ 6.0 \times 10^{-3} \\ \vdots \\ 1.0 \times 10^{-2} \\ 2.0 \times 10^{-2} \\ \vdots \\ 1.0 \times 10^{-1} \\ 2.0 \times 10^{-1} \\ \vdots \\ 6.0 \times 10^{-1} \end{bmatrix} \qquad r = \begin{bmatrix} 0.25 \\ 0.5 \\ 1. \\ 2. \\ 4. \\ 8. \\ 16. \end{bmatrix}$$

$$\sigma^{(1)} = \frac{0.2}{h}\left(1 - \frac{h}{2}\right)$$

0.2 is replaced by 0.05 for another set of calculation.

(d) Model D

$$\frac{\sigma^{(1)}_h}{\sigma^{(0)}_H} = 0.2, 0.05;\ d_2 = 0.5$$

$$h = \begin{bmatrix} 1.0 \times 10^{-3} \\ 2.0 \times 10^{-3} \\ \vdots \\ 1.0 \times 10^{-2} \\ 2.0 \times 10^{-2} \\ \vdots \\ 1.0 \times 10^{-1} \\ 2.0 \times 10^{-1} \\ 3.0 \times 10^{-1} \\ 4.0 \times 10^{-1} \end{bmatrix} \qquad r = \begin{bmatrix} 0.25 \\ 0.5 \\ 1. \\ 2. \\ 4. \\ 8. \\ 16. \end{bmatrix}$$

$$\sigma^{(1)} = \frac{0.2}{h}(0.5 - \frac{h}{2})$$

0.2 is replaced by 0.05 for another set of calculation.

It is found in the numerical calculations that if the second order term $\sigma^{(1)}$ is kept in the first order perturbation equation (refer to equations (82)) i.e.,

$$\frac{d^2\hat{V}^{(1)}}{dz^2} - k^2\hat{V}^{(1)} = -\frac{d \ln (\sigma_1)}{dz}\ \frac{d\hat{V}^{(0)}}{dz}\ , \qquad (86)$$

the results give better approximations than those obtained when the second order term $\sigma^{(1)}$ has been neglected. The first order correction obtained by solving (86) is

$$\hat{V}^{(1)}(0) = -\frac{I}{2\pi\sigma^{(0)}k}\left[\ln\left(\frac{\sigma_1}{\sigma^{(0)}}\right)\right]\left[\exp(-2kd_1)-\exp(-2kd_2)\right] . \qquad (87)$$

The corresponding correction for the second order equation can be found similarly. In the following series of figures (Figure 12 to 16) the first order results obtained through equation (87) for Models A, B and C are presented. More detailed calculations than indicated by Figure 12 to 16 have also been carried out. The figures give the results for the potential V in terms of the apparent resistivities for a Wenner electrode configuration. In the case of Model A and Model B, the first order perturbation results fail to give good approximations when $(\sigma^{(1)}h)/(\sigma^{(1)}H)$ exceeds 0.9 based on equation (87), and exceeds 0.4 based on equation (84). The second order results give little improvement except when $\sigma^{(1)}$ is small, then the second order approximation provides a clear improvement. In Model C and Model D $(\sigma^{(1)}h)/(\sigma^{(0)}H)$ has been chosen to be either 0.2 or 0.05, and the thickness of the perturbed layer (the layer with the electric conductivity $\sigma_1 = \sigma^{(0)} + \sigma^{(1)}$) is variable. The first order results show that the perturbation method fails to give good approximations when applying $\sigma^{(1)} \geq 5$ mho/m to equation (86) and $\sigma^{(1)} \geq 2$ mho/m to equation (84). The second order approximation does not give an improvement except

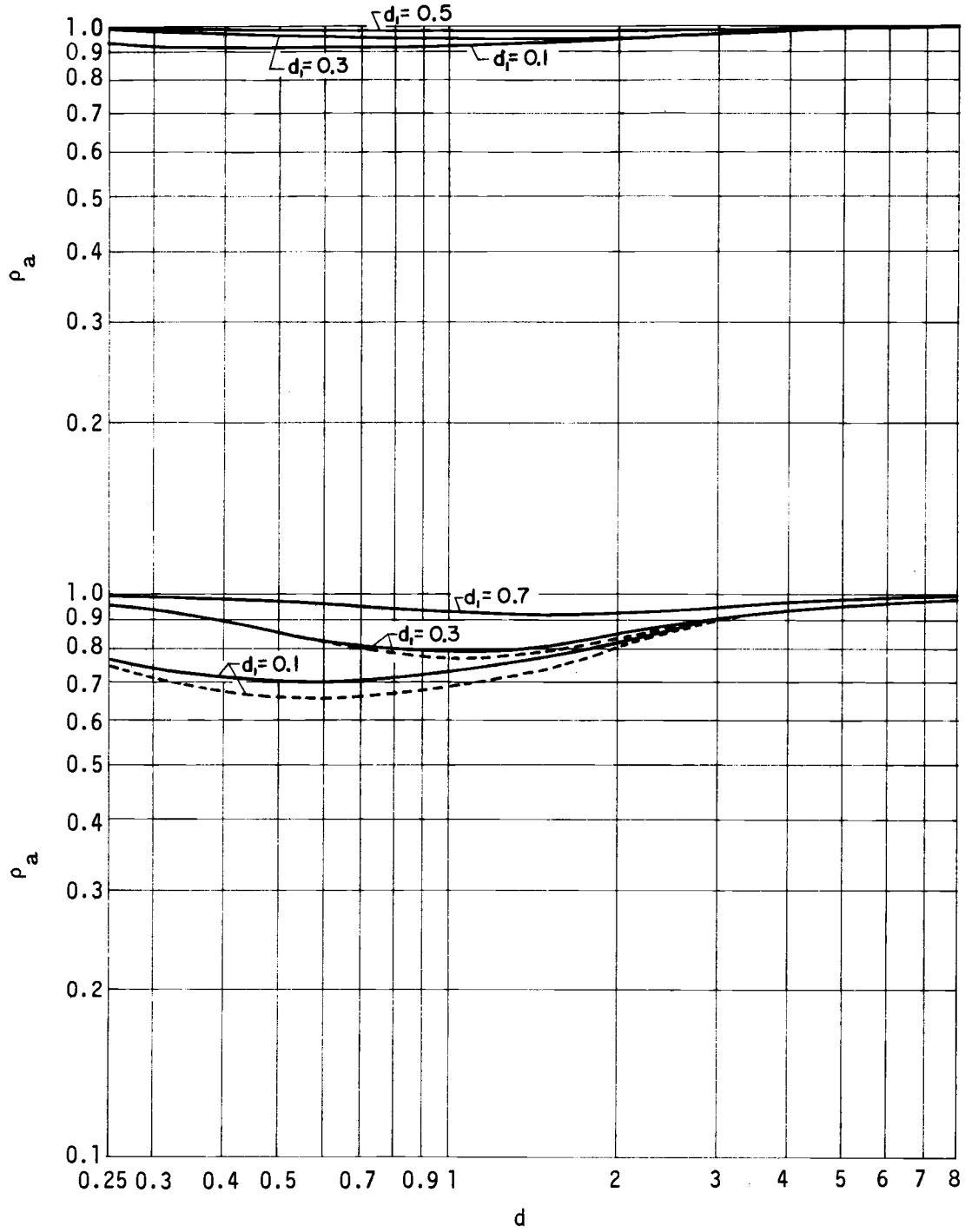

Figure 12. Apparent resistivity (ρ_a) curves calculated for Model A from the first order perturbation equations (dashed lines) compared with the corresponding ones calculated from the exact solutions (solid lines). Above: $\sigma^{(1)} = 0.1$, no difference can be seen in this plot. Below: $\sigma^{(1)} = 0.5$.

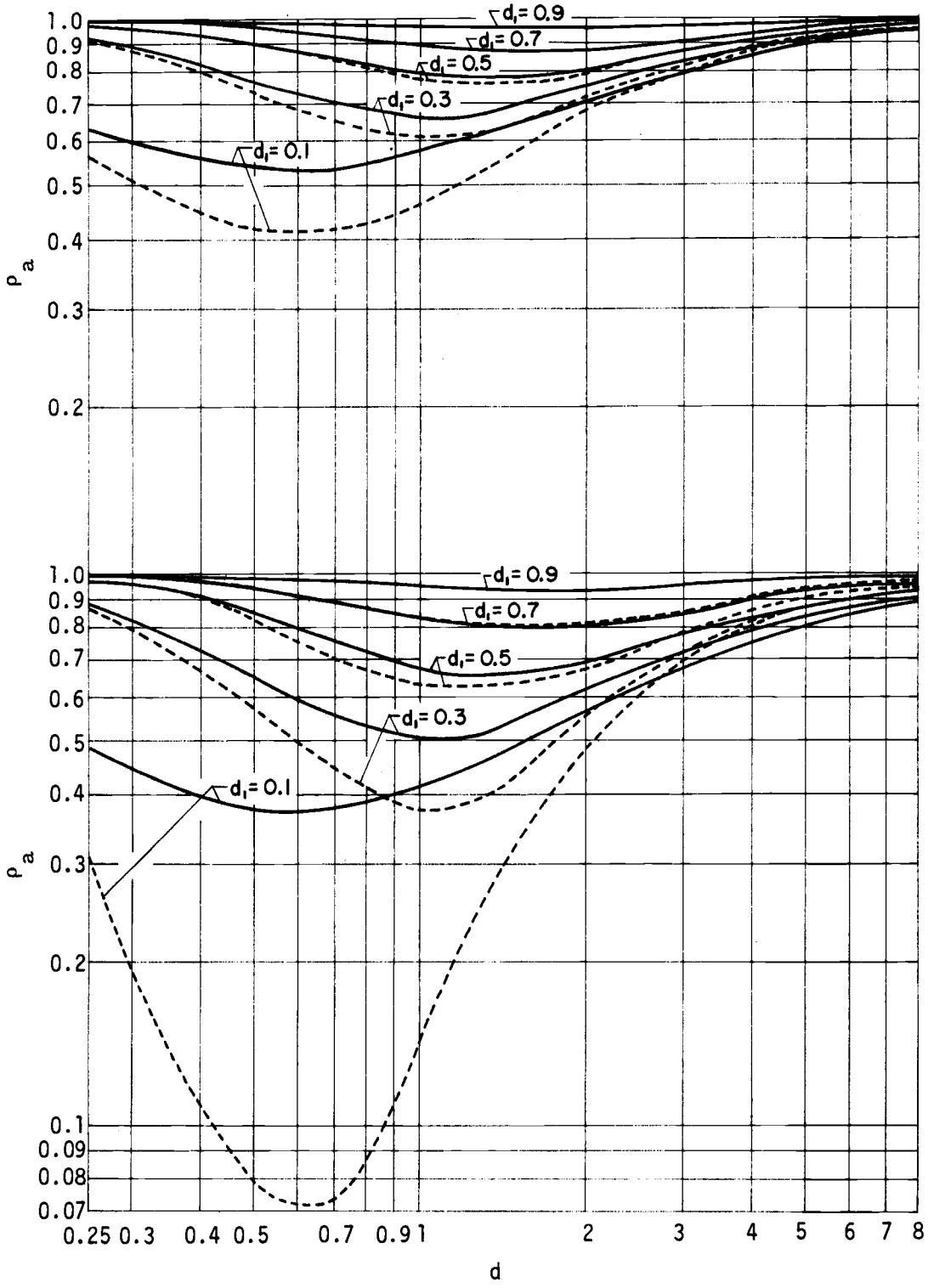

Figure 13. Apparent resistivity (ρ_a) curves calculated for Model A from the first order perturbation equations (dashed lines) compared with the corresponding ones calculated from the exact solutions (solid lines). Above: $\sigma^{(1)} = 1.0$. Below: $\sigma^{(1)} = 2.0$.

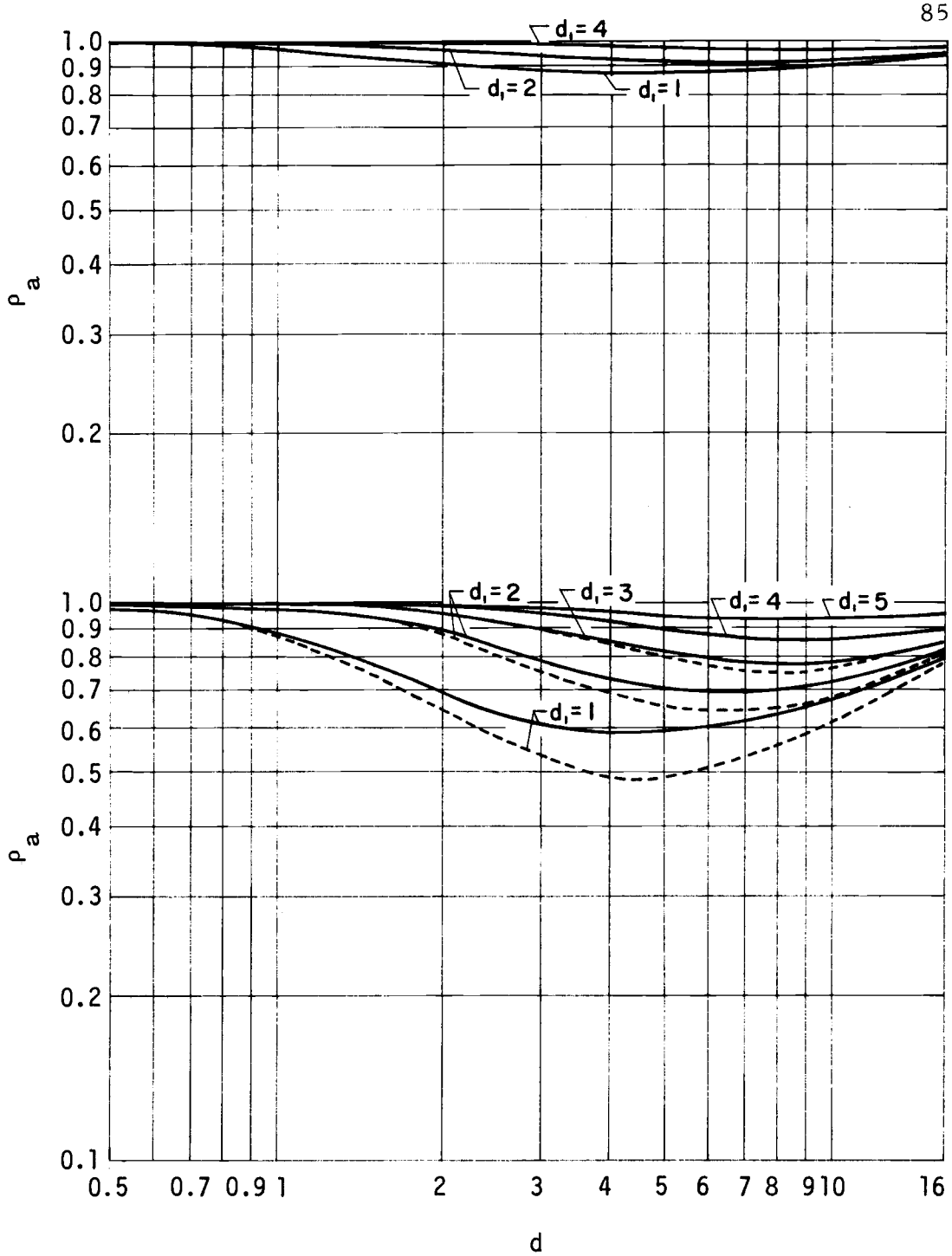

Figure 14. Apparent resistivity (ρ_a) curves calculated for Model B from the first order perturbation equations (dashed lines) compared with the corresponding ones calculated from the exact solutions (solid lines). Above: $\sigma^{(1)} = 0.4$, no difference can be seen in this plot. Below: $\sigma^{(1)} = 2.0$.

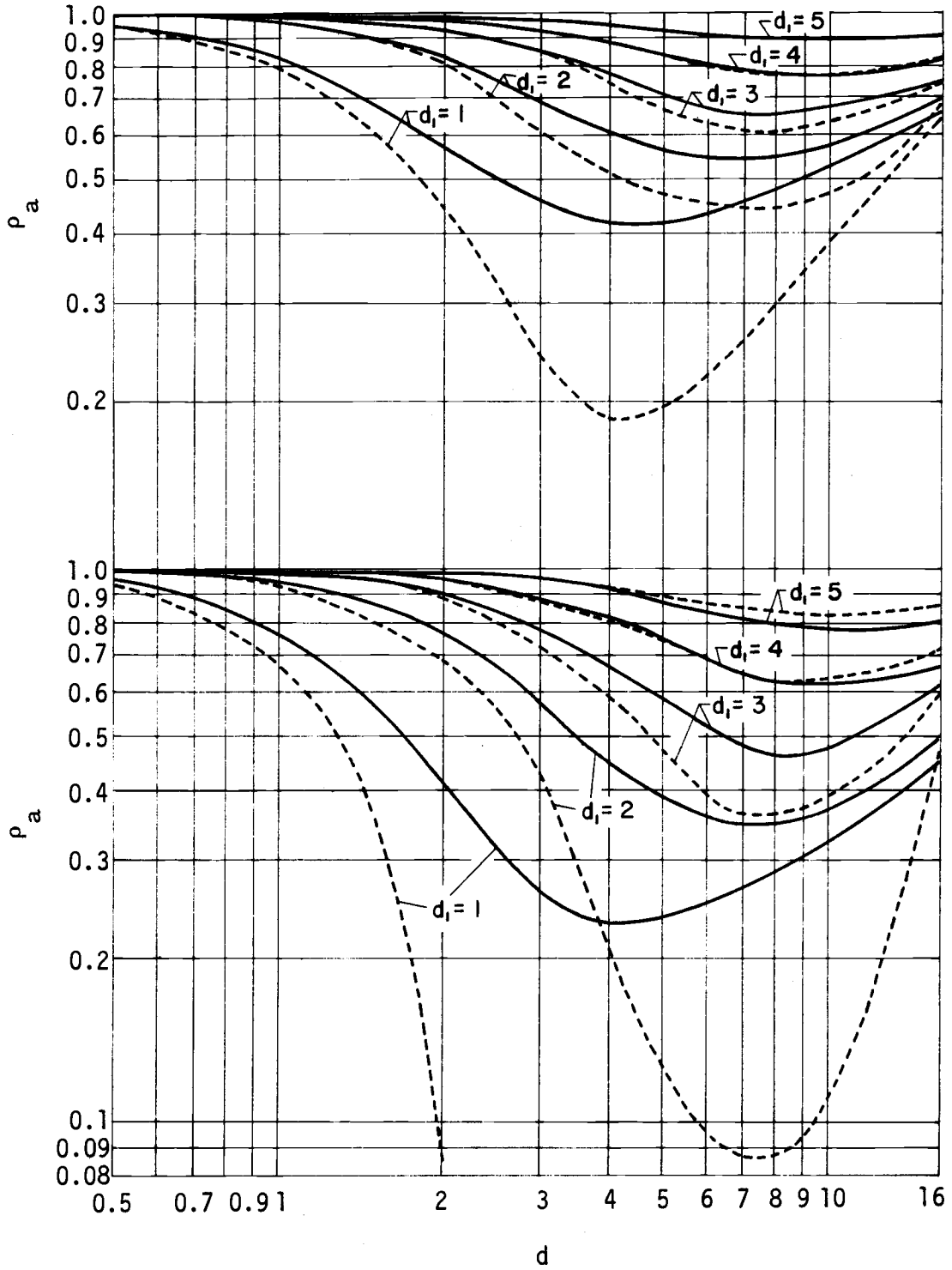

Figure 15. Apparent resistivity (ρ_a) curves calculated for Model B from the first order perturbation equations (dashed lines) compared with the corresponding ones calculated from the exact solutions (solid lines). Above: $\sigma^{(1)} = 4.0$. Below: $\sigma^{(1)} = 10.0$.

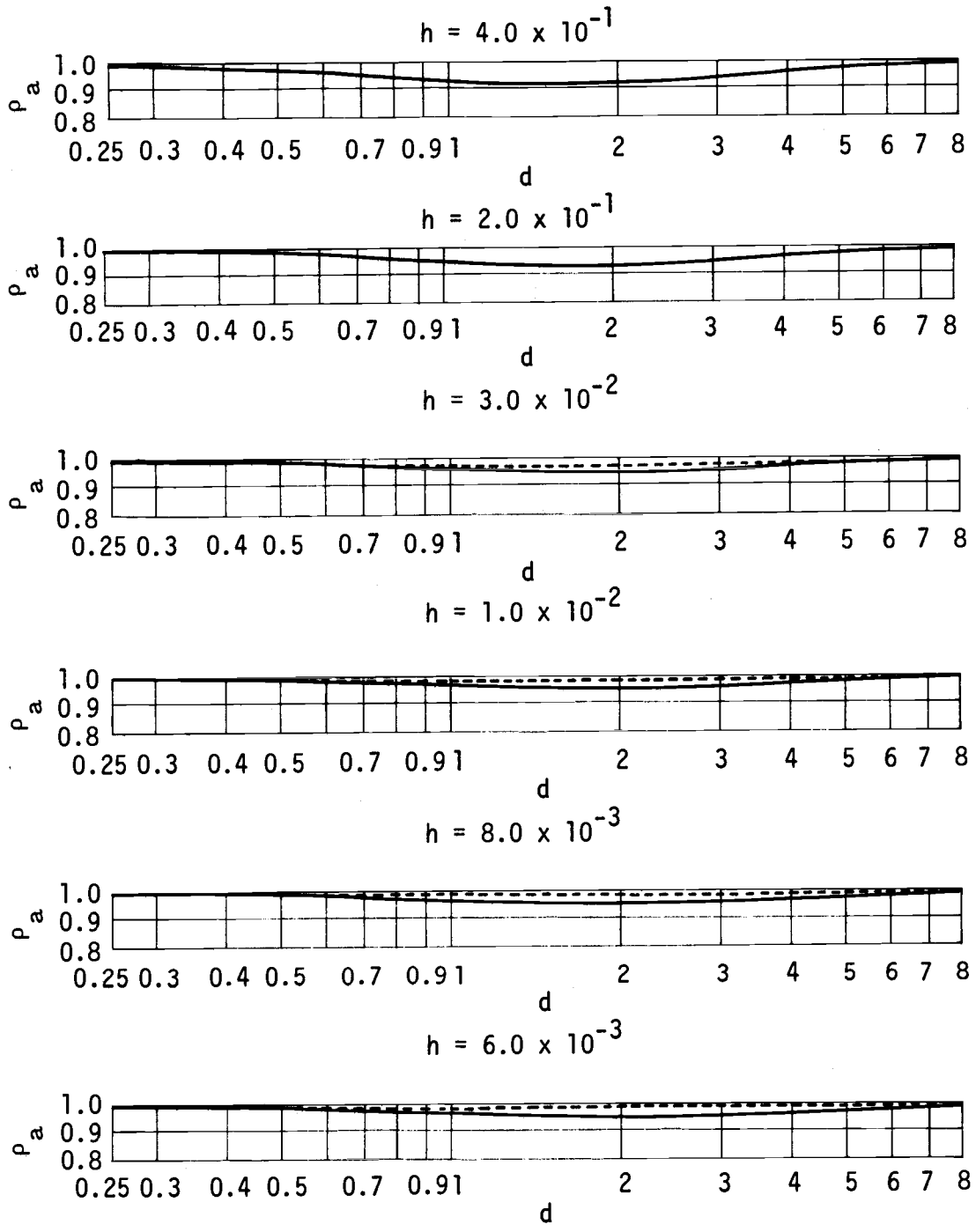

Figure 16. Apparent resistivity (ρ_a) curves calculated for Model C from the first order perturbation equations (dashed lines) compared with the corresponding ones calculated from the exact solutions (solid lines). These curves show the changes when the thickness of the perturbed layer is decreased. $(\sigma^{(1)}h)/(\sigma^{(0)}H) = 0.2$.

when $\sigma^{(1)}$ is small.

It is noted from equations (84), (85) and (82), (83) that the perturbation series for $\hat{V}(0)$ involves the powers of $\sigma^{(1)}/\sigma^{(0)}$ and the constant $[\exp(-2kd_1) - \exp(-2kd_2)]$. When either the ratio $\sigma^{(1)}/\sigma^{(0)}$ or the difference $d_1 - d_2$ is such that the magnitude of the successive terms in the perturbation series increases, the perturbation method fails to give a reasonable approximation.

(iii) Direct Method

Only the direct method using the first order perturbation approximation is considered in detail here. For higher order approximations the derivations are similar to this first order case. From the first order equation (see the second equation of equations (82)) one knows that

$$\hat{V}^{(1)}(z) = \int_0^z G_1 \left(-\frac{1}{\sigma^{(0)}} \frac{d\sigma^{(1)}}{dz'} \frac{d\hat{V}^{(0)}}{dz'}\right) dz' + \int_z^\infty G_2 \left(-\frac{1}{\sigma^{(0)}} \frac{d\sigma^{(1)}}{dz'} \frac{d\hat{V}^{(0)}}{dz'}\right) dz'$$

and when $z = 0$, on the surface of the ground,

$$\hat{V}^{(1)}(0) = \int_0^\infty G_2 \left(-\frac{1}{\sigma^{(0)}} \frac{d\sigma^{(1)}}{dz'} \frac{d\hat{V}^{(0)}}{dz'}\right) dz' \qquad (88)$$

where G_1, G_2 are the Green functions described in the last section. Inserting G_2 into (88) one obtains

$$\hat{V}^{(1)}(0) = -\frac{I}{2\pi\sigma^{(0)}k} \int_0^\infty \frac{1}{\sigma^{(0)}} \frac{d\sigma^{(1)}}{dz'} \exp(-2kz')\, dz' \quad . \qquad (89)$$

If the second order term $\sigma^{(1)}$ is retained in the first order equation, one obtains alternatively

$$\hat{V}^{(1)}(0) = -\frac{I}{2\pi\sigma^{(0)}k}\int_0^\infty \frac{d(\ln \sigma_1)}{dz'} \exp(-2kz')\, dz' \quad . \tag{90}$$

The right hand sides of equations (89) and (90) are Laplace transforms. Letting $2k = \eta$ in the equation (89) and performing the inverse Laplace transform, one obtains

$$\frac{d\sigma^{(1)}}{dz'} = -\left[\frac{\pi(\sigma^{(0)})^2}{I}\right]\frac{1}{2\pi i}\int_{c-i\infty}^{c+i\infty} \exp(\eta z')\, \eta \hat{V}^{(1)}(\eta, 0)\, d\eta \, . \tag{91}$$

When the same procedures are applied to equation (90), one obtains

$$\frac{d(\ln \sigma_1)}{dz'} = -\frac{\pi\sigma^{(0)}}{I}\frac{1}{2\pi i}\int_{c-i\infty}^{c+i\infty} \exp(\eta z')\eta\, \hat{V}^{(1)}(\eta, 0)\, d\eta \, . \tag{92}$$

Inserting $\hat{V}^{(1)}(0)$ from equation (84) into equation (89) we have

$$\int_0^\infty \exp(-\eta z')\frac{d\sigma^{(1)}}{dz'}\, dz' = \sigma^{(1)}[\exp(-\eta d_1) - \exp(-\eta d_2)] .$$

Following an integration by parts we obtain

$$\int_0^\infty \sigma^{(1)}(z') \exp(-\eta z')\, dz' = \sigma^{(1)}\{\frac{1}{\eta}[\exp(-\eta d_1) - \exp(-\eta d_2)]\} \, . \tag{93}$$

If we assume that $\sigma^{(1)}$ is a known constant, then $\sigma^{(1)}(z')$ can be obtained by the inverse Laplace transform analytically;

$$\sigma^{(1)}(z') = \sigma^{(1)}[\mathbb{1}(z' - d_1) - \mathbb{1}(z' - d_2)] \tag{94}$$

where $\mathbb{1}$ is the unit step function. This is the character of a three-

layer conductivity model (see diagram on p. 80). Applying the method of Piessens for the numerical inversion of the Laplace transform to equation (93), we obtain results which deviate from those of equation (94). This is attributed to the limited number of terms used in the Gaussian quadrature integration formula and the approximations involved in the inversion technique. Two examples given below will show the characteristics of the method when applied to equation (93). The first involving a two-layer case is the inversion of the equation

$$\int_0^\infty \sigma^{(1)}(z') \exp(-\eta z')\, dz' = \frac{\sigma^{(1)}}{\eta} \exp(-3.2\eta).$$

The result of $\sigma^{(1)}(z')$ is shown in Figure 17 by a dashed line and the solid line represents the correct result.

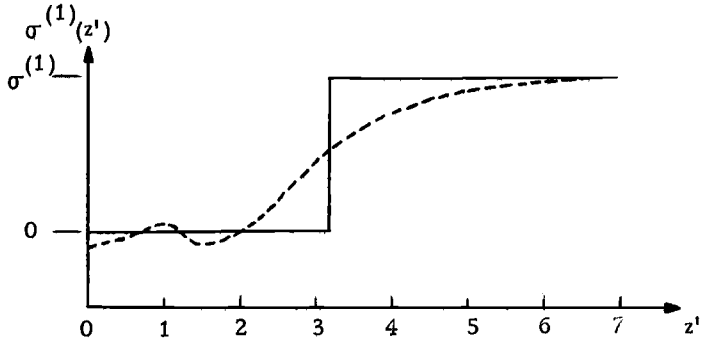

Figure 17. Approximate conductivity distribution for a two-layer case obtained from the numerical inversion of the Laplace transform compared with the correct result.

The second example involving a three-layer case is the inversion of the equation

$$\int_0^\infty \sigma^{(1)}(z') \exp(-\eta z')\, dz' = \frac{\sigma^{(1)}}{\eta} [\exp(-\eta) - \exp(-3.5\eta)] \quad .$$

The result is shown in Figure 18. The dashed and the solid lines have the same meanings as described in the first example above.

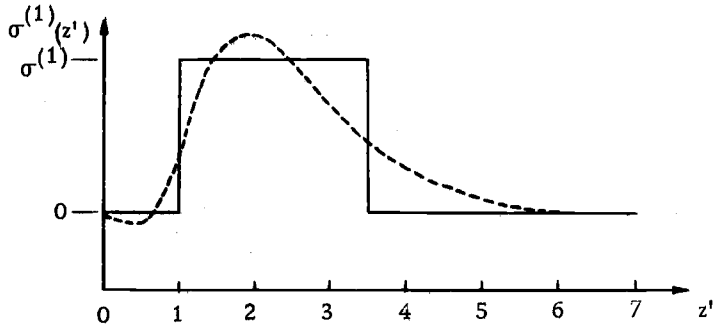

Figure 18. Approximate conductivity distribution for a three-layer case obtained from the numerical inversion of the Laplace transform compared with the correct result.

The approximate conductivity distributions shown in Figures 17 and 18 have been obtained by numerical inversions of the Laplace transformations. Obviously, the approximations to the conductivity distributions are only moderately good. The difficulty here is mainly with the numerical inversion, and better results can hardly be expected unless a greatly increased computational effort is devoted to the problem. In principle, the numerical inversion of Laplace transformation is an improperly posed problem which requires the continuation of a function of a complex variable from known values on the real axis into the complex plane. Formally, the continuation would be carried out on the basis of a Taylor series which requires that the derivatives of the function of all orders are known. In practice, this ideal situation cannot be realized. Moreover, all digitized data

include errors which are amplified in the inversion procedure. In this light, the results in Figure 17 and 18 are quite acceptable. Moreover, the integrated conductivity of the second layer in the three-layer case has been obtained with fairly good accuracy.

In the case when d_1 and d_2 are known the value of $\sigma^{(1)}$ can be found from equation (84) directly;

$$\sigma^{(1)} = \frac{2\pi(\sigma^{(0)})^2 k}{I} \frac{\hat{V}^{(1)}(0)}{\exp(-2kd_2) - \exp(-2kd_1)} .$$

Equations (89) and (90) can also be obtained by simply letting $a = 0$ in equation (72). As already mentioned in (vi) of the last section the theorem by Erdélyi is not a necessary condition for the direct method to work at the present situation.

Conclusion

In the second part of this thesis, the perturbation method is applied to the interpretation of D. C. conduction field data. An example from the three-layer case is discussed and worked out. The derivations indicate that there are no principal difficulties in applying the perturbation method in the D. C. conduction case provided certain basic conditions are satisfied, namely that the perturbation conductivities be small compared to the zero order conductivity. However, the final step in computations involves the numerical inversion of a Laplace transformation. This is an improperly posed problem where

computational and observational errors are greatly enhanced. This inversion is the main computational difficulty in applying the perturbation method to the inversion of D. C. conduction field data.

BIBLIOGRAPHY

Abramovitz, M. and I. A. Stegun. 1961. Handbook of mathematical functions. Dover Publications, Inc. New York. 1046 p.

Ames, L. D. 1902. Evaluation of slowly convergent series. Annals of Mathematics, series 2, vol. 3, pp. 185-192.

Ballance, J., J. A. Baughman and L. Ochs. 1971. OS-3 ARAND SYSTEM: Documentation and Examples. volume II, ccr-71-01. 238 p.

Bellman, R., R. E. Kalaba, and J. A. Lockett. 1966. Numerical inversion of the Laplace transform: applications to biology, economics, engineering, and physics. American Elsevier Publishing Company, Inc. New York. 249 p.

Bromwich, T. J. I'A. 1926. An introduction to the theory of infinite series. Macmillan and Co., Ltd. London. 535 p.

Bubnov, I. G. 1931. Report on the works of Professor Timoschenko which were awarded the Zhuranskii prize. Symposium of the Institute of Communication Engineers (Sborn. inta inzh. putei soobshch.). No. 81, All Union Special Planning Office (SPB).

Chan, S. H. 1970. A study on the direct interpretation of resistivity data measured by a Wenner electrode configuration. Geophysical Prospecting 18:215-235.

Collatz, L. 1960. The numerical treatment of differential equations. Springer-Verlag, Berlin, Göttingen, Heidelberg. 568 p.

Compagnie Generale de Geophysique, La. 1955. Abaques de sondage electrique (Curves of electric profiling). Geophysical Prospecting v. 3, supp. no. 3, 7 p. Many charts for three-layer case with explanation of Schlumberger configuration.

Cooley, J. W., P. A. W. Lewis and P. D. Welch. 1967. Application of the Fast Fourier Transform to computation of fourier integrals, fourier series, and convolution integrals. IEEE Transactions on Audio and Electroacoustics, vol. AV-15, no. 2, pp. 79-84.

Cooley, J. W. and J. W. Tukey. 1965. An algorithm for the machine calculation of complex Fourier series. Mathematics of Computation 19:297-301.

Courant, R. and D. Hilbert. 1953. Methoden der mathematischen Physik. I. English translation (with addition by Courant) published as Methods of Mathematical Physics by Interscience, New York.

_____. 1962. Methoden der mathematischen Physik. II. English translation published as Methods of Mathematical Physics by Interscience, New York.

Davis, P. and P. Rabinowitz. 1956. Abscissas and weights for Gaussian quadratures of high order. NBS Journal of Research, v. 56, Research Paper Z645, pp. 35-37.

Dubner, H. and J. Abate. 1968. Numerical inversion of Laplace transforms by relating them to the finite Fourier Cosine transform. Journal of the Association for Computing Machinery vol. 15, no. 1, pp. 115-123.

Duff, G. F. D. and D. Naylor. 1966. Differential equations of applied mathematics. John Wiley & Sons, Inc. New York, London, Sydney. 423 p.

Erdélyi, A. 1956. Asymptotic expansions. Dover Publications, Inc., New York. 108 p.

Erdélyi, A., W. Magnus, F. Oberhettinger, F. G. Tricomi. 1953. Higher transcendental functions. Volume II. New York, Toronto, London, McGraw-Hill Book Company, Inc. 396 p.

Fofonoff, N. P. 1962. Dynamics of ocean currents in The sea, volume 1, Physical Oceanography. Interscience Publishers, John Wiley & Sons, New York, London, pp. 323-395.

Friedrichs, K. O. 1938. Über die Spektralzerlegung eines Integraloperators. Mathematische Annalen 115:249-272.

_____. 1948. On the perturbation of continuous spectra. Communications on Pure and Applied Mathematics 1:361-406.

_____. 1965. Perturbation of spectra in Hilbert Space. American Mathematical Society, Providence, Rhode Island. 178 p.

Fritsch, J. and H. J. Zschau. 1969. A new semi-direct method for the interpretation of geoelectrical sounding graphs. Presented at 31st Meeting of the European Association of Exploration Geophysicists, Venice, May 1969.

Galerkin, B. G. 1915. Rods and plates. Series occurring in various questions concerning the elastic equilibrium of rods and plates. (Sterzhni i plastiny. Ryady v nekotorykh voprosakh uprogogo ravnovesiya sterzhnei i plastin.) Engineering Bulletin (Vestnik inzhenerov) 19:897-908.

Grant, F. S. and G. F. West. 1965. Interpretation theory in applied geophysics. McGraw-Hill Book Company. New York, St. Louis, San Francisco, Toronto, London, Sydney. 584 p.

Hansen, W. 1962. Tides. in The sea, volume 1, Physical Oceanography. Interscience Publishers, John Wiley & Sons, New York, London. pp. 764-801.

Harvard University, Computation Laboratory 1947. Annals, v. 3: Tables of the Bessel functions of the first kind of orders zero and one. Harvard University Press, Cambridge, Massachusetts.

Isaacs, J. D., J. L. Reid, Jr., G. B. Schick and R. A. Schwartzlose. 1966. Near-bottom currents measured in 4 kilometers depth off the Baja California coast. Journal of Geophysical Research 71(18):4297-4303.

Kato, T. 1951. On the convergence of the perturbation method. Journal of Faculty of Science, University of Tokyo, Sect. I. 6:145-226.

_____. 1966. Perturbation theory for linear operators. Springer-Verlag, New York Inc. 592 p.

Koefoed, O. 1965. Direct methods of interpreting resistivity observations. Geophysical Prospecting 13:568-592.

_____. 1966. The direct interpretation of resistivity observations made with a Wenner electrode configuration. Geophysical Prospecting 14:71-79.

Korgen, B. J., G. Bodvarsson and L. D. Kulm. 1970. Current speeds near the ocean floor west of Oregon. Deep-Sea Research 17:353-357.

Kunetz, G. and J. P. Rocroi. 1970. Traitement automatique des sondages electriques. (Automatic processing of electrical soundings) Geophysical Prospecting 18:157-198.

Lamb, Sir Horace. 1932. Hydrodynamics. Dover Publications, New York. 738 p.

Lanczos, C. 1956. Applied analysis. Prentice-Hall. Englewood Cliffs, New Jersey. 539 p.

Langer, R. E. 1933. An inverse problem in differential equations. American Mathematical Society Bulletin, ser. 2, 29:814-820. (see also 42:747-754. 1936).

Larsen, J. C. 1968[1]. Electric and magnetic fields induced by deep sea tides. Geophysical Journal of Royal Astronomical Society 16:47-70.

Larsen, J. C. 1968[2]. Long waves along a single-step topography in a semi-infinite uniformly rotating ocean. Journal of Marine Research, v. 27, no. 1, pp. 1-6.

Lee, T. 1972. A general technique for the direct interpretation of resistivity data over two-dimensional structures. Geophysical Prospecting 20:847-859.

Longman, I. M. 1956. Note on a method for computing infinite integrals of oscillatory functions. Cambridge Philosophical Society, Proceeding 52:764-768.

_____. 1957. Tables for the rapid and accurate numerical evaluation of certain infinite integrals involving Bessel functions. Mathematical Tables and Other Aids to Computation 11:166-180.

Mikhlin, S. G. 1952. The problem of the minimum of a quadratic functional (Problema minimuma kvadratichnogo junktsionala). Gostekhizdat. Translated by A. Feinstein. 1965. Holden-Day, Inc. San Francisco, London, Amsterdam. 155 p.

_____. 1964. Variational methods in mathematical physics. Translated by Boddington. Pergamon Press, Oxford, Edinburgh, London, New York, Paris, Frankfurt. 584 p.

_____ and K. L. Smolitskiy. 1967. Approximate methods for solution of differential and integral equations. American Elsevier Publishing Company Inc. New York. 308 p.

Milne, W. E. 1949. Numerical calculus. Princeton University Press. Princeton, New Jersey. 393 p.

Mooers, C. N. K. 1970. The interaction of an internal tide with the frontal zone in a coastal upwelling region. Ph. D. Thesis. Corvallis, Oregon State University. 480 p.

Mooney, H. M. and W. W. Wetzel. 1956. The potentials about a point electrode and apparent resistivity curves. Minneapolis, University of Minnesota Press.

Morse, P. M. and H. Feshbach. 1953. Methods of theoretical physics. 2 volumes. McGraw-Hill. New York, Toronto, London. 1978 p.

Munk, W., F. Snodgrass and M. Wimbush. 1970. Tides off-shore: Transition from California coastal to deep-sea waters. Geophysical Fluid Dynamics 1:161-235.

NBS Applied Mathematics Series, No. 37. 1954. Tables of Functions and of Zeros of Functions. U. S. Government Printing Office, Washington, D. C. 211 p.

Nowroozi, A. A., M. Ewing, J. E. Nafe and M. Fleigel. 1968. Deep ocean current and its correlation with the ocean tide off the coast of northern California. Journal of Geophysical Research 73(6):1921-1932.

Ochs, L., J. A. Baughman and J. Ballance. 1970. OS-3 ARAND SYSTEM: Documentation and Examples. volume I, CCY-70-4. 158 p.

Paul, M. K. 1968. A note on the direct interpretation of resistivity profiles for Wenner electrode configuration. Geophysical Prospecting 16:159-162.

Pekeris, C. L. 1940. Direct method of interpretation in resistivity prospecting. Geophysics 5:31-42.

Pekeris, C. L. and Y. Accad. 1969. Solution of Laplace's equations for the M_2 tide in the world oceans. Philosophical Transactions, Royal Society of London, Series A 265:413-436.

Piessens, R. 1969. Numerical inversion of the Laplace Transform. IEEE Transactions on Automatic Control, Correspondence, June, 1969 volume AC-14, pp. 299-301.

Rayleigh, Lord. 1926. The theory of sound. Volume I. Macmillan and Co., Ltd. London. 480 p.

Rellich, F. 1937[1]. Störungstheorie der Spektralzerlegung, I. Mathematische Annalen 113:600-619.

_____. 1937[2]. Störungstheorie der Spektralzerlegung, II. Mathematische Annalen 113:677-685.

_____. 1939. Störungstheorie der Spektralzerlegung, III. Mathematische Annalen 116:555-570.

_____. 1940. Störungstheorie der Spektralzerlegung, IV. Mathematische Annalen 117:356-382.

_____. 1942. Störungstheorie der Spektralzerlegung, V. Mathematische Annalen 118:462-484.

_____. 1953. Perturbation theory of eigenvalue problems. Lecture Notes, New York University, 164 p.

Ritz, W. 1908. Über eine neue Methode zur Lösung gewisser variations-probleme der mathematischen Physik. Journal für die reine und angewandte Mathematik 135:1-61.

_____. 1911. Gesammelte Werke. Œuvres. Publiées par la Société Suisse de Physique. Gauthier-Villars. Paris. 541 p.

Roman, I. 1941. Superposition in the interpretation of two-layer earth resistivity curves: U. S. Geological Survey Bulletin, 927-A. 18 p. GA 6302.

Schrödinger, E. 1928. Collected papers on wave mechanics. English translation. Blackie & Son limited. London and Glasgow. 146 p.

Slichter, L. B. 1933. Interpretation of resistivity prospecting for horizontal structure. Physics 4:307-322 (and p. 407).

Stefanesco, S. and C. and M. Schlumberger. 1930. Sur la distribution electrique potentielle autour d'une prise de terre ponctuelle dans un terrain a couches horizontales homogenes et isotropes. Journal de Physique et le Radium 7:132-140.

Titchmarsh, E. C. 1949. Some theorems on perturbation theory. Proceeding of Royal Society of London, ser. A, 200:34-46.

_____. 1950. Some theorems on perturbation theory. II. Proceeding of Royal Society of London, ser. A, 201:473-479.

Tomaschek, R. 1957. Tides of the solid earth. in Encyclopedia of Physics, Edited by S. Flügge, volume XLVIII Geophysics II. Group editor J. Bartels. Springer-Verlag, Berlin, Göttingen, Heidelberg. pp. 775-845.

Van Nostrand, R. G. and K. L. Cook. 1966. Interpretation of resistivity data. Geological Survey Professional Paper 499. United States Government Printing Office, Washington. 310 p.

Vozoff, K. 1956. Numerical resistivity analysis. Geophysics 23:536-556.

Weierstrass, K. 1895. Über das sogenannte Dirichlet'sche Prinzip. Matematische Werke v. K. Weierstrass, vol. 2, pp. 49-54. Mayer & Müller, Berlin.

Wetzel, W. W. and H. V. McMurry. 1937. A set of curves to assist in the interpretation of the three-layer resistivity problem. Geophysics 2:329-341.